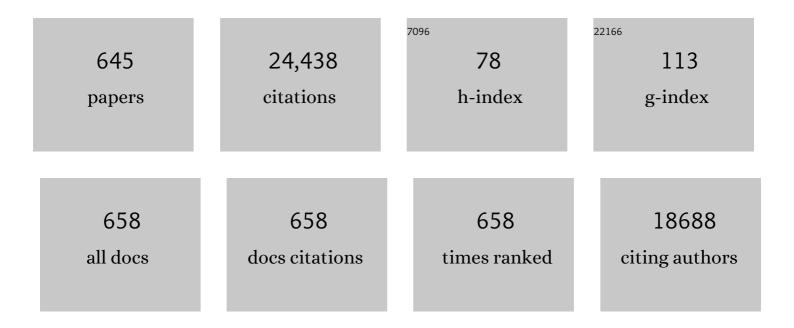
List of Publications by Year in descending order

Source: https://exaly.com/author-pdf/368269/publications.pdf Version: 2024-02-01



#	Article	IF	CITATIONS
1	Phase control of WC–Co hardmetal using additive manufacturing technologies. Powder Metallurgy, 2022, 65, 13-21.	1.7	13
2	Synthesis of <scp>MnSe</scp> @C yolkâ€shell nanospheres via a water vaporâ€assisted strategy for use as anode in sodiumâ€ion batteries. International Journal of Energy Research, 2022, 46, 2500-2511.	4.5	16
3	Metal sulfoselenide solid solution embedded in porous hollow carbon nanospheres as effective anode material for potassium-ion batteries with long cycle life and enhanced rate performance. Chemical Engineering Journal, 2022, 428, 131051.	12.7	18
4	Deliberate introduction of mesopores into microporous activated carbon toward efficient Se cathode of <scp>Naâ^'Se</scp> batteries. International Journal of Energy Research, 2022, 46, 3396-3408.	4.5	6
5	Doubleâ€shell and yolkâ€shell structured <scp>ZnSe</scp> â€carbon nanospheres as anode materials for highâ€performance potassiumâ€ion batteries. International Journal of Energy Research, 2022, 46, 3539-3553.	4.5	8
6	A 3D Porous Inverse Opal Ni Structure on a Cu Current Collector for Stable Lithiumâ€Metal Batteries. Batteries and Supercaps, 2022, 5, e202100257.	4.7	5
7	Aerosolâ€assisted synthesis of bimetallic nanoparticleâ€loaded bambooâ€like Nâ€doped carbon nanotubes as an efficient bifunctional oxygen catalyst for Znâ€air batteries. International Journal of Energy Research, 2022, 46, 5215-5225.	4.5	8
8	Novel synthetic strategy for a nanostructured metal hydroxysulfideâ€C and its initial electrochemical investigation as a new anode material for potassiumâ€ion batteries. International Journal of Energy Research, 2022, 46, 6323-6336.	4.5	2
9	Porous nitrogen-doped graphene nanofibers comprising metal organic framework-derived hollow and ultrafine layered double metal oxide nanocrystals as high-performance anodes for lithium-ion batteries. Journal of Power Sources, 2022, 523, 231030.	7.8	26
10	Investigating the role of metals loaded on nitrogen-doped carbon-nanotube electrodes in electroenzymatic alcohol dehydrogenation. Applied Catalysis B: Environmental, 2022, 307, 121195.	20.2	11
11	Investigation of the potassiumâ€ion storage mechanism of nickel selenide materials and rational design of nickel <scp>selenide </scp> yolkâ€shell structure for enhancing electrochemical properties. International Journal of Energy Research, 2022, 46, 5800-5810.	4.5	7
12	Carbon-Coated Three-Dimensional MXene/Iron Selenide Ball with Core–Shell Structure for High-Performance Potassium-Ion Batteries. Nano-Micro Letters, 2022, 14, 17.	27.0	61
13	Morphological and Electrochemical Properties of ZnMn2O4 Nanopowders and Their Aggregated Microspheres Prepared by Simple Spray Drying Process. Nanomaterials, 2022, 12, 680.	4.1	4
14	Electrochemical properties of yolkâ€shell structured cobalt hydroxy chloride arbon composite as an anode for lithiumâ€ion batteries. International Journal of Energy Research, 2022, 46, 9761-9770.	4.5	3
15	One-pot spray pyrolysis for core–shell structured Sn@SiOC anode nanocomposites that yield stable cycling in lithium-ion batteries. Applied Surface Science, 2022, 589, 152952.	6.1	7
16	Less energy-intensive synthesis of mesoporous multi-oriented graphite microspheres with low defect concentration for advanced potassium-ion battery anodes. Chemical Engineering Journal, 2022, 443, 136545.	12.7	10
17	A Novel Highâ€Performance TiO <sub>2â€x</sub> /TiO <sub>1â€y</sub> N <sub>y</sub> Coating Material for Silicon Anode in Lithiumâ€Ion Batteries. Small Methods, 2022, 6, .	8.6	9
18	Self-supported hierarchically porous 3D carbon nanofiber network comprising Ni/Co/NiCo2O4 nanocrystals and hollow N-doped C nanocages as sulfur host for highly reversible Li–S batteries. Chemical Engineering Journal, 2022, 446, 137141.	12.7	23

#	Article	IF	CITATIONS
19	Nanoconfined vanadium nitride in 3D porous reduced graphene oxide microspheres as high-capacity cathode for aqueous zinc-ion batteries. Chemical Engineering Journal, 2022, 446, 137266.	12.7	22
20	Macroporous vanadium dioxide–reduced graphene oxide microspheres: Cathode material with enhanced electrochemical kinetics for aqueous zinc-ion batteries. Applied Surface Science, 2022, 599, 153890.	6.1	9
21	Potassium-ion storage mechanism of MoS2-WS2-C microspheres and their excellent electrochemical properties. Chemical Engineering Journal, 2021, 408, 127278.	12.7	37
22	General strategy for yolk-shell nanospheres with tunable compositions by applying hollow carbon nanospheres. Chemical Engineering Journal, 2021, 406, 126840.	12.7	9
23	A General Solution to Mitigate Water Poisoning of Oxide Chemiresistors: Bilayer Sensors with Tb <sub>4</sub> O <sub>7</sub> Overlayer. Advanced Functional Materials, 2021, 31, 2007895.	14.9	33
24	Rational synthesis of uniform yolk–shell Ni–Fe bimetallic sulfide nanoflakes@porous carbon nanospheres as advanced anodes for high-performance potassium-/sodium-ion batteries. Chemical Engineering Journal, 2021, 417, 127963.	12.7	32
25	Ultrasonic spray pyrolysis for air-stable copper particles and their conductive films. Acta Materialia, 2021, 206, 116569.	7.9	16
26	MOF-Derived CoSe2@N-Doped Carbon Matrix Confined in Hollow Mesoporous Carbon Nanospheres as High-Performance Anodes for Potassium-Ion Batteries. Nano-Micro Letters, 2021, 13, 9.	27.0	83
27	Freestanding interlayers for Li–S batteries: design and synthesis of hierarchically porous N-doped C nanofibers comprising vanadium nitride quantum dots and MOF-derived hollow N-doped C nanocages. Journal of Materials Chemistry A, 2021, 9, 11651-11664.	10.3	45
28	Recent Advances in Heterostructured Anode Materials with Multiple Anions for Advanced Alkaliâ€ion Batteries. Advanced Energy Materials, 2021, 11, 2003058.	19.5	60
29	Highly Selective Detection of Benzene and Discrimination of Volatile Aromatic Compounds Using Oxide Chemiresistors with Tunable Rhâ€īiO <sub>2</sub> Catalytic Overlayers. Advanced Science, 2021, 8, 2004078.	11.2	56
30	Remote Control of Timeâ€Regulated Stretching of Ligandâ€Presenting Nanocoils In Situ Regulates the Cyclic Adhesion and Differentiation of Stem Cells. Advanced Materials, 2021, 33, e2008353.	21.0	31
31	Magnetic Nanocoils: Remote Control of Timeâ€Regulated Stretching of Ligandâ€Presenting Nanocoils In Situ Regulates the Cyclic Adhesion and Differentiation of Stem Cells (Adv. Mater. 11/2021). Advanced Materials, 2021, 33, 2170084.	21.0	0
32	Uniquely structured iron hydroxide-carbon nanospheres with yolk-shell and hollow structures and their excellent lithium-ion storage performances. Applied Surface Science, 2021, 542, 148637.	6.1	6
33	Initial investigation of bimetal hydroxysulfide as a new anode material for efficient sodium-ion storage. Chemical Engineering Journal, 2021, 410, 128401.	12.7	6
34	Synthesis of yolkâ€shellâ€structured iron monosulfideâ€carbon microspheres and understanding of their conversion reaction for potassiumâ€ion storage. International Journal of Energy Research, 2021, 45, 14910-14919.	4.5	11
35	Synthesis of threeâ€dimensional Co/ CoO /Nâ€doped carbon nanotube composite for zinc air battery. International Journal of Energy Research, 2021, 45, 16091-16101.	4.5	4
36	Yolkâ€Shellâ€Structured Nanospheres with Goat Pupilâ€Like Sâ€Doped SnSe Yolk and Hollow Carbonâ€Shell Configuration as Anode Material for Sodiumâ€Ion Storage. Small Methods, 2021, 5, e2100302.	8.6	17

#	Article	IF	CITATIONS
37	Immunoregulation of Macrophages by Controlling Winding and Unwinding of Nanohelical Ligands. Advanced Functional Materials, 2021, 31, 2103409.	14.9	19
38	A strategy for fabricating three-dimensional porous architecture comprising metal oxides/CNT as highly active and durable bifunctional oxygen electrocatalysts and their application in rechargeable Zn-air batteries. Chemical Engineering Journal, 2021, 414, 128815.	12.7	13
39	Novel synthesis method of cobalt hydroxycarbonate hydrateâ€reduced graphene oxide composite microspheres for lithiumâ€ion battery anode. International Journal of Energy Research, 2021, 45, 20302.	4.5	1
40	Nâ€doped <scp> carbonâ€coated CoSe <sub>2</sub> </scp> nanocrystals anchored on twoâ€dimensional <scp>MXene</scp> nanosheets for efficient electrochemical sodium―and <scp>potassiumâ€ion</scp> storage. International Journal of Energy Research, 2021, 45, 17738-17748.	4.5	35
41	Electrochemical Effect of Cokesâ€Derived Activated Carbon with Partially Graphitic Structure for Hybrid Supercapacitors. ChemElectroChem, 2021, 8, 3621-3628.	3.4	2
42	Boosting the Electrochemical Performance of V <sub>2</sub> O <sub>3</sub> by Anchoring on Carbon Nanotube Microspheres with Macrovoids for Ultrafast and Long‣ife Aqueous Zincâ€Ion Batteries. Small Methods, 2021, 5, e2100578.	8.6	25
43	Metalâ€organic frameworks derived <scp> FeSe <sub>2</sub> </scp> @C nanorods interconnected by Nâ€doped graphene nanosheets as advanced anode materials for Naâ€ion batteries. International Journal of Energy Research, 2021, 45, 20909-20920.	4.5	20
44	Magnetic Control and Realâ€Time Monitoring of Stem Cell Differentiation by the Ligand Nanoassembly. Small, 2021, 17, e2102892.	10.0	22
45	Hybrid Structure of TiO2-Graphitic Carbon as a Support of Pt Nanoparticles for Catalyzing Oxygen Reduction Reaction. Catalysts, 2021, 11, 1196.	3.5	4
46	Exploration of cobalt selenite–carbon composite porous nanofibers as anode for sodium-ion batteries and unveiling their conversion reaction mechanism. Journal of Materials Science and Technology, 2021, 89, 24-35.	10.7	18
47	New strategy to synthesize optimal cobalt diselenide@hollow mesoporous carbon nanospheres for highly efficient hydrogen evolution reaction. Chemical Engineering Journal, 2021, 424, 130341.	12.7	20
48	Hierarchically porous nanofibers comprising multiple core–shell Co3O4@graphitic carbon nanoparticles grafted within N-doped CNTs as functional interlayers for excellent Li–S batteries. Chemical Engineering Journal, 2021, 426, 130805.	12.7	49
49	Electrospun MOF-based ZnSe nanocrystals confined in N-doped mesoporous carbon fibers as anode materials for potassium ion batteries with long-term cycling stability. Chemical Engineering Journal, 2021, 425, 131651.	12.7	35
50	One-dimensional porous nanostructure composed of few-layered MoSe2 nanosheets and highly densified-entangled-N-doped CNTs as anodes for Na ion batteries. Chemical Engineering Journal, 2021, 425, 129051.	12.7	25
51	Macroporous microspheres consisting of thickness-controlled bamboo-like CNTs and flower-like Co <sub>3</sub> O <sub>4</sub> nanoparticles as highly efficient bifunctional oxygen electrocatalysts for Zn–air batteries. Journal of Materials Chemistry A, 2021, 9, 25160-25167.	10.3	13
52	Nitrogen-Doped and Carbon-Coated Activated Carbon as a Conductivity Additive-Free Electrode for Supercapacitors. Energies, 2021, 14, 7629.	3.1	0
53	Metal-Ion-Intercalated MXene Nanosheet Films for NH <sub>3</sub> Gas Detection. ACS Applied Nano Materials, 2021, 4, 14249-14257.	5.0	26
54	Scalable green synthesis of hierarchically porous carbon microspheres by spray pyrolysis for high-performance supercapacitors. Chemical Engineering Journal, 2020, 382, 122805.	12.7	40

#	Article	IF	CITATIONS
55	N-doped carbon coated Ni-Mo sulfide tubular structure decorated with nanobubbles for enhanced sodium storage performance. Chemical Engineering Journal, 2020, 383, 123112.	12.7	16
56	Preparation of activated carbon decorated with carbon dots and its electrochemical performance. Journal of Industrial and Engineering Chemistry, 2020, 82, 383-389.	5.8	16
57	Design of house centipede-like MoC–Mo2C nanorods grafted with N-doped carbon nanotubes as bifunctional catalysts for high-performance Li–O2 batteries. Chemical Engineering Journal, 2020, 384, 123344.	12.7	27
58	Structural combination of polar hollow microspheres and hierarchical N-doped carbon nanotubes for high-performance Li–S batteries. Nanoscale, 2020, 12, 2142-2153.	5.6	21
59	Giant-miscanthus-derived activated carbon and its application to lithium sulfur batteries. Carbon Letters, 2020, 30, 477-484.	5.9	10
60	Hierarchical Tubular‣tructured MoSe <sub>2</sub> Nanosheets/Nâ€Doped Carbon Nanocomposite with Enhanced Sodium Storage Properties. ChemSusChem, 2020, 13, 1546-1555.	6.8	45
61	Towards an efficient anode material for Li-ion batteries: understanding the conversion mechanism of nickel hydroxy chloride with Li- ions. Journal of Materials Chemistry A, 2020, 8, 1939-1946.	10.3	34
62	Uniquely structured quaternary metal oxide polyhedra as efficient anode materials for lithium-ion batteries. Applied Surface Science, 2020, 509, 144918.	6.1	5
63	Biotransformation of methane into methanol by methanotrophs immobilized on coconut coir. Bioresource Technology, 2020, 297, 122433.	9.6	50
64	Three-dimensional porous pitch-derived carbon coated Si nanoparticles-CNT composite microsphere with superior electrochemical performance for lithium ion batteries. Journal of Alloys and Compounds, 2020, 821, 153224.	5.5	38
65	Encapsulation of Se into Hierarchically Porous Carbon Microspheres with Optimized Pore Structure for Advanced Na–Se and K–Se Batteries. ACS Nano, 2020, 14, 13203-13216.	14.6	86
66	Conversion reaction mechanism of cobalt telluride-carbon composite microspheres synthesized by spray pyrolysis process for K-ion storage. Applied Surface Science, 2020, 529, 147140.	6.1	37
67	Porous SnO <sub>2</sub> /C Nanofiber Anodes and LiFePO <sub>4</sub> /C Nanofiber Cathodes with a Wrinkle Structure for Stretchable Lithium Polymer Batteries with High Electrochemical Performance. Advanced Science, 2020, 7, 2001358.	11.2	22
68	Conversion Reaction Mechanism of Ultrafine Bimetallic Coâ€Fe Selenides Embedded in Hollow Mesoporous Carbon Nanospheres and Their Excellent Kâ€Ion Storage Performance. Small, 2020, 16, e2002345.	10.0	54
69	Amorphous Cobalt Selenite Nanoparticles Decorated on a Graphitic Carbon Hollow Shell for High-Rate and Ultralong Cycle Life Lithium-Ion Batteries. ACS Sustainable Chemistry and Engineering, 2020, 8, 17707-17717.	6.7	15
70	Photo-immobilization of pseudozwitterionic polymers with balanced electrical charge for developing anti-coagulation surfaces. Journal of Industrial and Engineering Chemistry, 2020, 91, 263-272.	5.8	2
71	Efficient strategy for hollow carbon nanospheres embedded with nickel hydroxide nanocrystals and their excellent lithium-ion storage performances. Scripta Materialia, 2020, 188, 112-117.	5.2	10
72	Conversion Reaction Mechanism for Yolkâ€Shellâ€Structured Iron Tellurideâ€C Nanospheres and Exploration of Their Electrochemical Performance as an Anode Material for Potassiumâ€Ion Batteries. Small Methods, 2020, 4, 2000556.	8.6	38

#	Article	IF	CITATIONS
73	Sodiumâ€Ion Batteries: Golden Bristlegrassâ€Like Hierarchical Graphene Nanofibers Entangled with Nâ€Doped CNTs Containing CoSe <sub>2</sub> Nanocrystals at Each Node as Anodes for Highâ€Rate Sodiumâ€Ion Batteries (Small 38/2020). Small, 2020, 16, 2070207.	10.0	1
74	Golden Bristlegrassâ€Like Hierarchical Graphene Nanofibers Entangled with Nâ€Doped CNTs Containing CoSe <sub>2</sub> Nanocrystals at Each Node as Anodes for Highâ€Rate Sodiumâ€Ion Batteries. Small, 2020, 16, e2003391.	10.0	58
75	Sodium-ion storage performances of MoS2 nanocrystals coated with N-doped carbon synthesized by flame spray pyrolysis. Applied Surface Science, 2020, 523, 146470.	6.1	11
76	The conversion reaction mechanism of bimetallic Ni–Fe hydroxycarbonate and its encapsulation in carbon nanospheres for achieving excellent Li-ion storage performance. Journal of Materials Chemistry A, 2020, 8, 12124-12133.	10.3	27
77	Enhanced Li-ion storage performance of novel tube-in-tube structured nanofibers with hollow metal oxide nanospheres covered with a graphitic carbon layer. Nanoscale, 2020, 12, 8404-8414.	5.6	9
78	Hierarchically Wellâ€Developed Porous Graphene Nanofibers Comprising Nâ€Doped Graphitic Câ€Coated Cobalt Oxide Hollow Nanospheres As Anodes for Highâ€Rate Liâ€Ion Batteries. Small, 2020, 16, e2002213.	10.0	46
79	Investigation of cobalt hydroxysulfide as a new anode material for Li-ion batteries and its conversion reaction mechanism with Li-ions. Chemical Engineering Journal, 2020, 401, 126121.	12.7	22
80	Fibrous network of highly integrated carbon nanotubes/MoO3 composite bundles anchored with MoO3 nanoplates for superior lithium ion battery anodes. Journal of Industrial and Engineering Chemistry, 2020, 83, 438-448.	5.8	33
81	Prussian blue analogue nanocubes with hollow interior and porous walls encapsulated within reduced graphene oxide nanosheets and their sodium-ion storage performances. Chemical Engineering Journal, 2020, 393, 124606.	12.7	31
82	Lithium ion storage mechanism exploration of copper selenite as anode materials for lithium-ion batteries. Journal of Alloys and Compounds, 2020, 827, 154309.	5.5	20
83	A New Strategy for Detecting Plant Hormone Ethylene Using Oxide Semiconductor Chemiresistors: Exceptional Gas Selectivity and Response Tailored by Nanoscale Cr <sub>2</sub> O <sub>3</sub> Catalytic Overlayer. Advanced Science, 2020, 7, 1903093.	11.2	49
84	Methylbenzene sensors using Ti-doped NiO multiroom spheres: Versatile tunability on selectivity, response, sensitivity, and detection limit. Sensors and Actuators B: Chemical, 2020, 308, 127730.	7.8	28
85	Porous nanofibers comprised of hollow SnO2 nanoplate building blocks for high-performance lithium ion battery anode. Materials Characterization, 2020, 161, 110099.	4.4	15
86	Electrochemical reaction mechanism of amorphous iron selenite with ultrahigh rate and excellent cyclic stability performance as new anode material for lithium-ion batteries. Chemical Engineering Journal, 2020, 389, 124350.	12.7	42
87	Carbon-templated strategy toward the synthesis of dense and yolk-shell multi-component transition metal oxide cathode microspheres for high-performance Li ion batteries. Journal of Power Sources, 2020, 461, 228115.	7.8	13
88	Amorphous iron oxide–selenite composite microspheres with a yolk–shell structure as highly efficient anode materials for lithium-ion batteries. Nanoscale, 2020, 12, 10790-10798.	5.6	26
89	Metal Oxide Gas Sensors with Au Nanocluster Catalytic Overlayer: Toward Tuning Gas Selectivity and Response Using a Novel Bilayer Sensor Design. ACS Applied Materials & Interfaces, 2019, 11, 32169-32177.	8.0	83
90	Advances in the synthesis and design of nanostructured materials by aerosol spray processes for efficient energy storage. Nanoscale, 2019, 11, 19012-19057.	5.6	30

#	Article	IF	CITATIONS
91	Recent Advances in Aerosolâ€Assisted Spray Processes for the Design and Fabrication of Nanostructured Metal Chalcogenides for Sodiumâ€Ion Batteries. Chemistry - an Asian Journal, 2019, 14, 3127-3140.	3.3	19
92	Aerosol-assisted synthesis of porous and hollow carbon-carbon nanotube composite microspheres as sulfur host materials for high-performance Li-S batteries. Applied Surface Science, 2019, 495, 143637.	6.1	21
93	Yolk–shell-structured microspheres composed of N-doped-carbon-coated NiMoO <sub>4</sub> hollow nanospheres as superior performance anode materials for lithium-ion batteries. Nanoscale, 2019, 11, 631-638.	5.6	41
94	Uniquely structured composite microspheres of metal sulfides and carbon with cubic nanorooms for highly efficient anode materials for sodium-ion batteries. Journal of Materials Chemistry A, 2019, 7, 2636-2645.	10.3	50
95	Unique structured microspheres with multishells comprising graphitic carbon-coated Fe <sub>3</sub> O <sub>4</sub> hollow nanopowders as anode materials for high-performance Li-ion batteries. Journal of Materials Chemistry A, 2019, 7, 15766-15773.	10.3	61
96	Synthesis of carbonaceous/carbon-free nanofibers consisted of Co3V2O8 nanocrystals for lithium-ion battery anode with ultralong cycle life. Electrochimica Acta, 2019, 313, 48-58.	5.2	26
97	A MOF-mediated strategy for constructing human backbone-like CoMoS <sub>3</sub> @N-doped carbon nanostructures with multiple voids as a superior anode for sodium-ion batteries. Journal of Materials Chemistry A, 2019, 7, 13751-13761.	10.3	85
98	Pitch-derived yolk-shell-structured carbon microspheres as efficient sulfur host materials and their application as cathode material for Li–S batteries. Chemical Engineering Journal, 2019, 373, 382-392.	12.7	41
99	Superior lithium-ion storage performances of SnO2 powders consisting of hollow nanoplates. Journal of Alloys and Compounds, 2019, 797, 380-389.	5.5	10
100	Yolk–shell-structured manganese oxide/nitride composite powders comprising cobalt-nanoparticle-embedded nitrogen-doped carbon nanotubes as cathode catalysts for long-life-cycle lithium–oxygen batteries. Chemical Engineering Journal, 2019, 373, 86-94.	12.7	22
101	Uniquely structured Sb nanoparticle-embedded carbon/reduced graphene oxide composite shell with empty voids for high performance sodium-ion storage. Chemical Engineering Journal, 2019, 373, 227-237.	12.7	39
102	Trimodally porous N-doped carbon frameworks with an interconnected pore structure as selenium immobilizers for high-performance Li-Se batteries. Materials Characterization, 2019, 151, 590-601.	4.4	16
103	New synthesis strategy for hollow NiO nanofibers with interstitial nanovoids prepared via electrospinning using camphene for anodes of lithium-ion batteries. Journal of Industrial and Engineering Chemistry, 2019, 77, 76-82.	5.8	26
104	Synthesis Process of CoSeO <sub>3</sub> Microspheres for Unordinary Liâ€ion Storage Performances and Mechanism of Their Conversion Reaction with Li ions. Small, 2019, 15, e1901320.	10.0	49
105	Multi-channel-contained few-layered MoSe2 nanosheet/N-doped carbon hybrid nanofibers prepared using diethylenetriamine as anodes for high-performance sodium-ion batteries. Journal of Industrial and Engineering Chemistry, 2019, 75, 100-107.	5.8	39
106	Mesoporous CoSe2 nanoclusters threaded with nitrogen-doped carbon nanotubes for high-performance sodium-ion battery anodes. Chemical Engineering Journal, 2019, 370, 1008-1018.	12.7	131
107	Pitch-derived carbon coated SnO2–CoO yolk–shell microspheres with excellent long-term cycling and rate performances as anode materials for lithium-ion batteries. Chemical Engineering Journal, 2019, 369, 726-735.	12.7	40
108	Highly integrated and interconnected CNT hybrid nanofibers decorated with α-iron oxide as freestanding anodes for flexible lithium polymer batteries. Journal of Materials Chemistry A, 2019, 7, 12480-12488.	10.3	19

#	Article	IF	CITATIONS
109	RGO/sAC composites as electrode materials for supercapacitors to enhance electrochemical performance. Journal of Physics and Chemistry of Solids, 2019, 131, 69-78.	4.0	7
110	Hierarchical yolk-shell CNT-(NiCo)O/C microspheres prepared by one-pot spray pyrolysis as anodes in lithium-ion batteries. Chemical Engineering Journal, 2019, 368, 438-447.	12.7	28
111	The effect of ILs as co-salts in electrolytes for high voltage supercapacitors. Scientific Reports, 2019, 9, 1180.	3.3	22
112	Carbon microspheres with micro- and mesopores synthesized via spray pyrolysis for high-energy-density, electrical-double-layer capacitors. Chemical Engineering Journal, 2019, 365, 193-200.	12.7	33
113	Investigation of Binary Metal (Ni, Co) Selenite as Liâ€lon Battery Anode Materials and Their Conversion Reaction Mechanism with Li Ions. Small, 2019, 15, e1905289.	10.0	51
114	Strategy for synthesizing mesoporous NiO polyhedra with empty nanovoids via oxidation of NiSe polyhedra by nanoscale Kirkendall diffusion and their superior lithium-ion storage performance. Applied Surface Science, 2019, 464, 597-605.	6.1	12
115	Nickel vanadate microspheres with numerous nanocavities synthesized by spray drying process as an anode material for Li-ion batteries. Journal of Alloys and Compounds, 2019, 780, 326-333.	5.5	24
116	A Saltâ€Templated Strategy toward Hollow Iron Selenidesâ€Graphitic Carbon Composite Microspheres with Interconnected Multicavities as Highâ€Performance Anode Materials for Sodiumâ€Ion Batteries. Small, 2019, 15, e1803043.	10.0	108
117	SiO2 microparticles with carbon nanotube-derived mesopores as an efficient support for enzyme immobilization. Chemical Engineering Journal, 2019, 359, 1252-1264.	12.7	154
118	Quorum sensing inhibitors as antipathogens: biotechnological applications. Biotechnology Advances, 2019, 37, 68-90.	11.7	215
119	Fabrication of bimodal micro-mesoporous amorphous carbon-graphitic carbon-reduced graphene oxide composite microspheres prepared by pilot-scale spray drying and their application in supercapacitors. Carbon, 2019, 144, 591-600.	10.3	24
120	Coral-Like Yolk–Shell-Structured Nickel Oxide/Carbon Composite Microspheres for High-Performance Li-Ion Storage Anodes. Nano-Micro Letters, 2019, 11, 3.	27.0	54
121	Mesoporous Nb2O5 microspheres with filled and yolk-shell structure as anode materials for lithium-ion batteries. Journal of Alloys and Compounds, 2019, 776, 722-730.	5.5	22
122	Germanium Nanoparticle-Dispersed Reduced Graphene Oxide Balls Synthesized by Spray Pyrolysis for Li-Ion Battery Anode. Journal of the Korean Ceramic Society, 2019, 56, 65-70.	2.3	9
123	Metal-Organic-Framework-Derived N-Doped Hierarchically Porous Carbon Polyhedrons Anchored on Crumpled Graphene Balls as Efficient Selenium Hosts for High-Performance Lithium–Selenium Batteries. ACS Applied Materials & Interfaces, 2018, 10, 16531-16540.	8.0	64
124	Superior electrochemical properties of micron-sized aggregates of (Co0.5Fe0.5)3O4 hollow nanospheres and graphitic carbon. Chemical Engineering Journal, 2018, 346, 351-360.	12.7	5
125	Synthesis of hierarchical structured Fe2O3 rod clusters with numerous empty nanovoids via the Kirkendall effect and their electrochemical properties for lithium-ion storage. Journal of Materials Chemistry A, 2018, 6, 8462-8469.	10.3	31
126	Scalable synthesis of NiMoO4 microspheres with numerous empty nanovoids as an advanced anode material for Li-ion batteries. Journal of Power Sources, 2018, 379, 278-287.	7.8	64

#	Article	IF	CITATIONS
127	Mesoporous graphitic carbon microspheres with a controlled amount of amorphous carbon as an efficient Se host material for Li–Se batteries. Journal of Materials Chemistry A, 2018, 6, 4152-4160.	10.3	34
128	Design and Synthesis of Spherical Multicomponent Aggregates Composed of Core–Shell, Yolk–Shell, and Hollow Nanospheres and Their Lithiumâ€lon Storage Performances. Small, 2018, 14, e1703957.	10.0	25
129	Repeated batch methanol production from a simulated biogas mixture using immobilized Methylocystis bryophila. Energy, 2018, 145, 477-485.	8.8	42
130	Synthesis of cross-linked protein-metal hybrid nanoflowers and its application in repeated batch decolorization of synthetic dyes. Journal of Hazardous Materials, 2018, 347, 442-450.	12.4	145
131	MOF-Templated N-Doped Carbon-Coated CoSe <sub>2</sub> Nanorods Supported on Porous CNT Microspheres with Excellent Sodium-Ion Storage and Electrocatalytic Properties. ACS Applied Materials & Interfaces, 2018, 10, 17203-17213.	8.0	164
132	Dual Role of Multiroom-Structured Sn-Doped NiO Microspheres for Ultrasensitive and Highly Selective Detection of Xylene. ACS Applied Materials & Interfaces, 2018, 10, 16605-16612.	8.0	96
133	Design and synthesis of tube-in-tube structured NiO nanobelts with superior electrochemical properties for lithium-ion storage. Chemical Engineering Journal, 2018, 347, 889-899.	12.7	57
134	Multiroom-structured multicomponent metal selenide–graphitic carbon–carbon nanotube hybrid microspheres as efficient anode materials for sodium-ion batteries. Nanoscale, 2018, 10, 8125-8132.	5.6	35
135	Iron diselenide combined with hollow graphitic carbon nanospheres as a high-performance anode material for sodium-ion batteries. Chemical Engineering Journal, 2018, 339, 97-107.	12.7	48
136	Electrochemical properties of multicomponent oxide and selenide microspheres containing Co and Mo components with several tens of vacant nanorooms synthesized by spray pyrolysis. Chemical Engineering Journal, 2018, 333, 665-677.	12.7	30
137	Superior lithium-ion storage performances of carbonaceous microspheres with high electrical conductivity and uniform distribution of Fe and TiO ultrafine nanocrystals for Li-S batteries. Carbon, 2018, 126, 394-403.	10.3	13
138	An artificial synthetic pathway for acetoin, 2,3-butanediol, and 2-butanol production from ethanol using cell free multi-enzyme catalysis. Green Chemistry, 2018, 20, 230-242.	9.0	58
139	Design and synthesis of macroporous (Mn1/3Co2/3)O-carbon nanotubes composite microspheres as efficient catalysts for rechargeable Li-O2 batteries. Carbon, 2018, 128, 125-133.	10.3	24
140	Yolk–Shell Structured Assembly of Bamboo‣ike Nitrogenâ€Doped Carbon Nanotubes Embedded with Co Nanocrystals and Their Application as Cathode Material for Li–S Batteries. Advanced Functional Materials, 2018, 28, 1705264.	14.9	122
141	Three-dimensional macroporous CNTs microspheres highly loaded with NiCo2O4 hollow nanospheres showing excellent lithium-ion storage performances. Carbon, 2018, 128, 191-200.	10.3	38
142	Selenium-infiltrated metal–organic framework-derived porous carbon nanofibers comprising interconnected bimodal pores for Li–Se batteries with high capacity and rate performance. Journal of Materials Chemistry A, 2018, 6, 1028-1036.	10.3	103
143	Electrochemical properties of uniquely structured Fe2O3 and FeSe2/graphitic-carbon microrods synthesized by applying a metal-organic framework. Chemical Engineering Journal, 2018, 334, 2440-2449.	12.7	64
144	Hierarchical hollow microspheres grafted with Co nanoparticle-embedded bamboo-like N-doped carbon nanotube bundles as ultrahigh rate and long-life cathodes for rechargeable lithium-oxygen batteries. Chemical Engineering Journal, 2018, 334, 2500-2510.	12.7	30

#	Article	IF	CITATIONS
145	Mesoporous graphitic carbon-TiO2 composite microspheres produced by a pilot-scale spray-drying process as an efficient sulfur host material for Li-S batteries. Chemical Engineering Journal, 2018, 335, 600-611.	12.7	59
146	Rational design and synthesis of hierarchically structured SnO2 microspheres assembled from hollow porous nanoplates as superior anode materials for lithium-ion batteries. Nano Research, 2018, 11, 1301-1312.	10.4	32
147	Rattle-type porous Sn/C composite fibers with uniformly distributed nanovoids containing metallic Sn nanoparticles for high-performance anode materials in lithium-ion batteries. Nanoscale, 2018, 10, 21483-21491.	5.6	64
148	Three-dimensionally ordered mesoporous multicomponent (Ni, Mo) metal oxide/N-doped carbon composite with superior Li-ion storage performance. Nanoscale, 2018, 10, 18734-18741.	5.6	35
149	Carbon microspheres with well-developed micro- and mesopores as excellent selenium host materials for lithium–selenium batteries with superior performances. Journal of Materials Chemistry A, 2018, 6, 21410-21418.	10.3	16
150	Insights into Cell-Free Conversion of CO <sub>2</sub> to Chemicals by a Multienzyme Cascade Reaction. ACS Catalysis, 2018, 8, 11085-11093.	11.2	87
151	Improving the Electrochemical Performance of Lithium Metal Batteries with Hollow Shell Microspheres and Polypyrrole Vapor Phase-Coated LiV <sub>3</sub> O <sub>8</sub> Cathodes. Journal of the Electrochemical Society, 2018, 165, A2919-A2924.	2.9	3
152	Amorphous Molybdenum Sulfide on Three-Dimensional Hierarchical Hollow Microspheres Comprising Bamboo-like N-Doped Carbon Nanotubes as a Highly Active Hydrogen Evolution Reaction Catalyst. ACS Sustainable Chemistry and Engineering, 2018, 6, 12706-12715.	6.7	28
153	Structure-optimized CoP-carbon nanotube composite microspheres synthesized by spray pyrolysis for hydrogen evolution reaction. Journal of Alloys and Compounds, 2018, 763, 652-661.	5.5	32
154	Rational design of metal-organic framework-templated hollow NiCo2O4 polyhedrons decorated on macroporous CNT microspheres for improved lithium-ion storage properties. Chemical Engineering Journal, 2018, 349, 214-222.	12.7	49
155	Design and synthesis of interconnected hierarchically porous anatase titanium dioxide nanofibers as high-rate and long-cycle-life anodes for lithium-ion batteries. Nanoscale, 2018, 10, 13539-13547.	5.6	17
156	Highly efficient hierarchical multiroom-structured molybdenum carbide/carbon composite microspheres grafted with nickel-nanoparticle-embedded nitrogen-doped carbon nanotubes as air electrode for lithium-oxygen batteries. Chemical Engineering Journal, 2018, 351, 886-896.	12.7	28
157	Lithium-ion storage performances of sunflower-like and nano-sized hollow SnO <sub>2</sub> spheres by spray pyrolysis and the nanoscale Kirkendall effect. Nanoscale, 2018, 10, 13531-13538.	5.6	24
158	One-dimensional nanostructure comprising MoSe2 nanosheets and carbon with uniformly defined nanovoids as an anode for high-performance sodium-ion batteries. Chemical Engineering Journal, 2018, 351, 559-568.	12.7	82
159	Unique hollow NiO nanooctahedrons fabricated through the Kirkendall effect as anodes for enhanced lithium-ion storage. Chemical Engineering Journal, 2018, 354, 327-334.	12.7	43
160	Mesoporous reduced graphene oxide/WSe2 composite particles for efficient sodium-ion batteries and hydrogen evolution reactions. Applied Surface Science, 2018, 459, 309-317.	6.1	47
161	Rationally designed microspheres consisting of yolk–shell structured FeSe <sub>2</sub> –Fe <sub>2</sub> O <sub>3</sub> nanospheres covered with graphitic carbon for lithium-ion batteries. Journal of Materials Chemistry A, 2018, 6, 15182-15190.	10.3	42
162	Three-dimensional porous microspheres comprising hollow Fe2O3 nanorods/CNT building blocks with superior electrochemical performance for lithium ion batteries. Nanoscale, 2018, 10, 11150-11157.	5.6	46

#	Article	IF	CITATIONS
163	Superior Electrochemical Properties of Composite Microspheres Consisting of Hollow Fe <sub>2</sub> O <sub>3</sub> Nanospheres and Graphitic Carbon. ACS Sustainable Chemistry and Engineering, 2018, 6, 11759-11767.	6.7	13
164	Batteries: Synthesis of Uniquely Structured SnO <sub>2</sub> Hollow Nanoplates and Their Electrochemical Properties for Liâ€lon Storage (Adv. Funct. Mater. 4/2017). Advanced Functional Materials, 2017, 27, .	14.9	0
165	Protein–inorganic hybrid system for efficient his-tagged enzymes immobilization and its application in <scp>l</scp> -xylulose production. RSC Advances, 2017, 7, 3488-3494.	3.6	90
166	Electrochemical properties of amorphous GeO x -C composite microspheres prepared by a one-pot spray pyrolysis process. Ceramics International, 2017, 43, 5534-5540.	4.8	7
167	Aerosol synthesis of molybdenum diselenide–reduced graphene oxide composite with empty nanovoids and enhanced hydrogen evolution reaction performances. Chemical Engineering Journal, 2017, 315, 355-363.	12.7	43
168	MoSe <sub>2</sub> Embedded CNT-Reduced Graphene Oxide Composite Microsphere with Superior Sodium Ion Storage and Electrocatalytic Hydrogen Evolution Performances. ACS Applied Materials & Interfaces, 2017, 9, 10673-10683.	8.0	174
169	Alkali resistant Ni-loaded yolk-shell catalysts for direct internal reforming in molten carbonate fuel cells. Journal of Power Sources, 2017, 352, 1-8.	7.8	14
170	1-D nanostructure comprising porous Fe <sub>2</sub> O <sub>3</sub> /Se composite nanorods with numerous nanovoids, and their electrochemical properties for use in lithium-ion batteries. Journal of Materials Chemistry A, 2017, 5, 10632-10639.	10.3	42
171	Porous FeS nanofibers with numerous nanovoids obtained by Kirkendall diffusion effect for use as anode materials for sodium-ion batteries. Nano Research, 2017, 10, 897-907.	10.4	142
172	Electrochemical properties of P2-type Na 2/3 Ni 1/3 Mn 2/3 O 2 plates synthesized by spray pyrolysis process for sodium-ion batteries. Electrochimica Acta, 2017, 225, 86-92.	5.2	44
173	Rational Design and Synthesis of Extremely Efficient Macroporous CoSe <sub>2</sub> -CNT Composite Microspheres for Hydrogen Evolution Reaction. Small, 2017, 13, 1700068.	10.0	116
174	Excellent Li-ion storage performances of hierarchical SnO-SnO 2 composite powders and SnO nanoplates prepared by one-pot spray pyrolysis. Journal of Power Sources, 2017, 359, 363-370.	7.8	32
175	Yolk–shell-structured (Fe0.5Ni0.5)9S8 solid-solution powders: Synthesis and application as anode materials for Na-ion batteries. Nano Research, 2017, 10, 3178-3188.	10.4	44
176	Multicomponent (Mo, Ni) metal sulfide and selenide microspheres with empty nanovoids as anode materials for Na-ion batteries. Journal of Materials Chemistry A, 2017, 5, 8616-8623.	10.3	80
177	Unraveling the Issue of Ag Migration in Printable Source/Drain Electrodes Compatible with Versatile Solution-Processed Oxide Semiconductors for Printed Thin-Film Transistor Applications. ACS Applied Materials & Interfaces, 2017, 9, 14058-14066.	8.0	12
178	High microporosity of carbide-derived carbon prepared from a vacuum-treated precursor for energy storage devices. Carbon, 2017, 118, 327-338.	10.3	11
179	Eco-Friendly Composite of Fe <sub>3</sub> O <sub>4</sub> -Reduced Graphene Oxide Particles for Efficient Enzyme Immobilization. ACS Applied Materials & amp; Interfaces, 2017, 9, 2213-2222.	8.0	205
180	Carbon/two-dimensional MoTe <sub>2</sub> core/shell-structured microspheres as an anode material for Na-ion batteries. Nanoscale, 2017, 9, 1942-1950.	5.6	93

#	Article	IF	CITATIONS
181	Ultra-selective detection of sub-ppm-level benzene using Pd–SnO <sub>2</sub> yolk–shell micro-reactors with a catalytic Co <sub>3</sub> O <sub>4</sub> overlayer for monitoring air quality. Journal of Materials Chemistry A, 2017, 5, 1446-1454.	10.3	111
182	Synthesis of Uniquely Structured Yolk–Shell Metal Oxide Microspheres Filled with Nitrogenâ€Đoped Graphitic Carbon with Excellent Li–Ion Storage Performance. Small, 2017, 13, 1701585.	10.0	25
183	Rapid synthesis and decoration of reduced graphene oxide with gold nanoparticles by thermostable peptides for memory device and photothermal applications. Scientific Reports, 2017, 7, 10980.	3.3	84
184	Metal–organic framework-templated hollow Co3O4 nanosphere aggregate/N-doped graphitic carbon composite powders showing excellent lithium-ion storage performances. Materials Characterization, 2017, 132, 320-329.	4.4	33
185	Excellent sodium-ion storage performances of CoSe2 nanoparticles embedded within N-doped porous graphitic carbon nanocube/carbon nanotube composite. Chemical Engineering Journal, 2017, 328, 546-555.	12.7	187
186	Metal–organic framework-derived CoSe <sub>2</sub> /(NiCo)Se <sub>2</sub> box-in-box hollow nanocubes with enhanced electrochemical properties for sodium-ion storage and hydrogen evolution. Journal of Materials Chemistry A, 2017, 5, 18823-18830.	10.3	213
187	Design and synthesis of Janus-structured mutually doped SnO <sub>2</sub> –Co <sub>3</sub> O <sub>4</sub> hollow nanostructures as superior anode materials for lithium-ion batteries. Journal of Materials Chemistry A, 2017, 5, 25319-25327.	10.3	49
188	A new general approach to synthesizing filled and yolk–shell structured metal oxide microspheres by applying a carbonaceous template. Nanoscale, 2017, 9, 17991-17999.	5.6	20
189	Synthesis of Uniquely Structured SnO <sub>2</sub> Hollow Nanoplates and Their Electrochemical Properties for Liâ€lon Storage. Advanced Functional Materials, 2017, 27, 1603399.	14.9	96
190	A strategy for ultrasensitive and selective detection of methylamine using p-type Cr2O3: Morphological design of sensing materials, control of charge carrier concentrations, and configurational tuning of Au catalysts. Sensors and Actuators B: Chemical, 2017, 240, 1049-1057.	7.8	52
191	Selenium-impregnated hollow carbon microspheres as efficient cathode materials for lithium-selenium batteries. Carbon, 2017, 111, 198-206.	10.3	58
192	Yolk–shell carbon microspheres with controlled yolk and void volumes and shell thickness and their application as a cathode material for Li–S batteries. Journal of Materials Chemistry A, 2017, 5, 988-995.	10.3	46
193	Dependence of Thermal and Electrochemical Properties of ceramic Coated Separators on the Ceramic Particle Size. Journal of the Korean Electrochemical Society, 2017, 20, 27-33.	0.1	1
194	Oneâ€Pot Synthesis of CoSe <sub><i>x</i></sub> –rGO Composite Powders by Spray Pyrolysis and Their Application as Anode Material for Sodiumâ€Ion Batteries. Chemistry - A European Journal, 2016, 22, 4140-4146.	3.3	124
195	Sodiumâ€lon Storage Properties of FeS–Reduced Graphene Oxide Composite Powder with a Crumpled Structure. Chemistry - A European Journal, 2016, 22, 2769-2774.	3.3	101
196	Highly Selective Xylene Sensor Based on NiO/NiMoO <sub>4</sub> Nanocomposite Hierarchical Spheres for Indoor Air Monitoring. ACS Applied Materials & Interfaces, 2016, 8, 34603-34611.	8.0	122
197	Preparation of Hollow Fe2O3 Nanorods and Nanospheres by Nanoscale Kirkendall Diffusion, and Their Electrochemical Properties for Use in Lithium-Ion Batteries. Scientific Reports, 2016, 6, 38933.	3.3	58
198	A highly efficient sorbitol dehydrogenase from Gluconobacter oxydans G624 and improvement of its stability through immobilization. Scientific Reports, 2016, 6, 33438.	3.3	42

#	Article	IF	CITATIONS
199	Superior electrochemical properties of SiO2-doped Co3O4 hollow nanospheres obtained through nanoscale Kirkendall diffusion for lithium-ion batteries. Journal of Alloys and Compounds, 2016, 680, 366-372.	5.5	15
200	Extremely sensitive ethanol sensor using Pt-doped SnO2 hollow nanospheres prepared by Kirkendall diffusion. Sensors and Actuators B: Chemical, 2016, 234, 353-360.	7.8	80
201	Role of the non-conserved amino acid asparagine 285 in the glycone-binding pocket of Neosartorya fischeri β-glucosidase. RSC Advances, 2016, 6, 48137-48144.	3.6	16
202	Superior Na-ion storage properties of high aspect ratio SnSe nanoplates prepared by a spray pyrolysis process. Nanoscale, 2016, 8, 11889-11896.	5.6	70
203	Sodium-ion storage performance of hierarchically structured (Co <sub>1/3</sub> Fe <sub>2/3</sub> )Se <sub>2</sub> nanofibers with fiber-in-tube nanostructures. Journal of Materials Chemistry A, 2016, 4, 15471-15477.	10.3	42
204	A New Strategy for Humidity Independent Oxide Chemiresistors: Dynamic Selfâ€Refreshing of In <sub>2</sub> O <sub>3</sub> Sensing Surface Assisted by Layerâ€byâ€Layer Coated CeO <sub>2</sub> Nanoclusters. Small, 2016, 12, 4229-4240.	10.0	195
205	Electrochemical properties of WO3-reduced graphene oxide composite powders prepared by one-pot spray pyrolysis process. Journal of Alloys and Compounds, 2016, 688, 647-653.	5.5	22
206	Iron Telluride-Decorated Reduced Graphene Oxide Hybrid Microspheres as Anode Materials with Improved Na-Ion Storage Properties. ACS Applied Materials & Interfaces, 2016, 8, 21343-21349.	8.0	71
207	Electrochemical properties of micron-sized Co3O4 hollow powders consisting of size controlled hollow nanospheres. Journal of Alloys and Compounds, 2016, 689, 554-563.	5.5	23
208	Large-scale production of spherical FeSe2-amorphous carbon composite powders as anode materials for sodium-ion batteries. Materials Characterization, 2016, 120, 349-356.	4.4	72
209	Graphitic Carbon-Coated FeSe2 Hollow Nanosphere-Decorated Reduced Graphene Oxide Hybrid Nanofibers as an Efficient Anode Material for Sodium Ion Batteries. Scientific Reports, 2016, 6, 23699.	3.3	127
210	Extremely Low-Cost, Scalable Oxide Semiconductors Employing Poly(acrylic acid)-Decorated Carbon Nanotubes for Thin-Film Transistor Applications. ACS Applied Materials & Interfaces, 2016, 8, 29858-29865.	8.0	4
211	Na-ion Storage Performances of FeSex and Fe2O3 Hollow Nanoparticles-Decorated Reduced Graphene Oxide Balls prepared by Nanoscale Kirkendall Diffusion Process. Scientific Reports, 2016, 6, 22432.	3.3	64
212	Applying Nanoscale Kirkendall Diffusion for Template-Free, Kilogram-Scale Production of SnO2 Hollow Nanospheres via Spray Drying System. Scientific Reports, 2016, 6, 23915.	3.3	30
213	First Introduction of NiSe2 to Anode Material for Sodium-Ion Batteries: A Hybrid of Graphene-Wrapped NiSe2/C Porous Nanofiber. Scientific Reports, 2016, 6, 23338.	3.3	150
214	Design and synthesis of multiroom-structured metal compounds–carbon hybrid microspheres as anode materials for rechargeable batteries. Nano Energy, 2016, 26, 466-478.	16.0	86
215	Highly Active and Stable Pt-Loaded Ce <sub>0.75</sub> Zr <sub>0.25</sub> O <sub>2</sub> Yolk–Shell Catalyst for Water–Gas Shift Reaction. ACS Applied Materials & Interfaces, 2016, 8, 17239-17244.	8.0	36
216	Phytoremediation of metal-contaminated soils by the hyperaccumulator canola (Brassica napus L.) and the use of its biomass for ethanol production. Fuel, 2016, 183, 107-114.	6.4	72

#	Article	IF	CITATIONS
217	Design and synthesis of metal oxide hollow nanopowders for lithium-ion batteries by combining nanoscale Kirkendall diffusion and flame spray pyrolysis. Ceramics International, 2016, 42, 5461-5471.	4.8	9
218	All-in-One Beaker Method for Large-Scale Production of Metal Oxide Hollow Nanospheres Using Nanoscale Kirkendall Diffusion. ACS Applied Materials & Interfaces, 2016, 8, 3800-3809.	8.0	15
219	Fullerene-like MoSe <sub>2</sub> nanoparticles-embedded CNT balls with excellent structural stability for highly reversible sodium-ion storage. Nanoscale, 2016, 8, 4209-4216.	5.6	131
220	Enhancement of methanol production from synthetic gas mixture by Methylosinus sporium through covalent immobilization. Applied Energy, 2016, 171, 383-391.	10.1	53
221	Trimodally porous SnO2 nanospheres with three-dimensional interconnectivity and size tunability: a one-pot synthetic route and potential application as an extremely sensitive ethanol detector. NPG Asia Materials, 2016, 8, e244-e244.	7.9	77
222	Highly sensitive and selective detection of ppb-level NO 2 using multi-shelled WO 3 yolk–shell spheres. Sensors and Actuators B: Chemical, 2016, 229, 561-569.	7.8	80
223	Electrochemical properties of CuO hollow nanopowders prepared from formless Cu–C composite via nanoscale Kirkendall diffusion process. Journal of Alloys and Compounds, 2016, 671, 74-83.	5.5	13
224	Large-scale aerosol-assisted synthesis of biofriendly Fe <sub>2</sub> O <sub>3</sub> yolk–shell particles: a promising support for enzyme immobilization. Nanoscale, 2016, 8, 6728-6738.	5.6	144
225	Hollow Cobalt Selenide Microspheres: Synthesis and Application as Anode Materials for Na-Ion Batteries. ACS Applied Materials & Interfaces, 2016, 8, 6449-6456.	8.0	130
226	Electrochemical properties of hollow copper (II) oxide nanopowders prepared by salt-assisted spray drying process applying nanoscale Kirkendall diffusion. Journal of Applied Electrochemistry, 2016, 46, 469-477.	2.9	6
227	Strategy for yolk-shell structured metal oxide-carbon composite powders and their electrochemical properties for lithium-ion batteries. Carbon, 2016, 100, 137-144.	10.3	35
228	One-pot Aerosol Synthesis of Carbon Nanotube-Zn2GeO4 Composite Microspheres for Enhanced Lithium-ion Storage Properties. Electrochimica Acta, 2016, 190, 766-774.	5.2	18
229	Electrochemical properties of core-shell structured NiO@SiO2 ultrafine nanopowders below 10 nm for lithium-ion storages. Electrochimica Acta, 2016, 190, 835-842.	5.2	9
230	Electrochemical Properties of Fiberâ€inâ€Tube―and Filledâ€Structured TiO <sub>2</sub> Nanofiber Anode Materials for Lithiumâ€Ion Batteries. Chemistry - A European Journal, 2015, 21, 11082-11087.	3.3	31
231	Superior Lithiumâ€ion Storage Properties of Mesoporous CuO–Reduced Graphene Oxide Composite Powder Prepared by a Twoâ€Step Sprayâ€Drying Process. Chemistry - A European Journal, 2015, 21, 9179-9184.	3.3	25
232	Polystyreneâ€Templated Aerosol Synthesis of MoS <sub>2</sub> –Amorphous Carbon Composite with Open Macropores as Battery Electrode. ChemSusChem, 2015, 8, 2260-2267.	6.8	32
233	Nanofibers Comprising Yolk-Shell Sn@void@SnO/SnO <sub>2</sub> and Hollow SnO/SnO <sub>2</sub> and SnO <sub>2</sub> Nanospheres via the Kirkendall Diffusion Effect and Their Electrochemical Properties. Small, 2015, 11, 4673-4681.	10.0	119
234	Electrochemical Properties of Yolk–Shell‣tructured Zn–Fe–S Multicomponent Sulfide Materials with a 1:2 Zn/Fe Molar Ratio. Chemistry - A European Journal, 2015, 21, 1429-1433.	3.3	16

#	Article	IF	CITATIONS
235	A Highly Efficient Recombinant Laccase from the Yeast Yarrowia lipolytica and Its Application in the Hydrolysis of Biomass. PLoS ONE, 2015, 10, e0120156.	2.5	50
236	Characterization of a Mannose-6-Phosphate Isomerase from Bacillus amyloliquefaciens and Its Application in Fructose-6-Phosphate Production. PLoS ONE, 2015, 10, e0131585.	2.5	15
237	Amorphous GeO <sub><i>x</i></sub> -Coated Reduced Graphene Oxide Balls with Sandwich Structure for Long-Life Lithium-Ion Batteries. ACS Applied Materials & amp; Interfaces, 2015, 7, 13952-13959.	8.0	63
238	Phase-pure β-NiMoO4 yolk-shell spheres for high-performance anode materials in lithium-ion batteries. Electrochimica Acta, 2015, 174, 102-110.	5.2	52
239	Enhanced Li+ storage properties of few-layered MoS2-C composite microspheres embedded with Si nanopowder. Nano Research, 2015, 8, 2492-2502.	10.4	27
240	Large-Scale Production of MoO 3 -Reduced Graphene Oxide Powders with Superior Lithium Storage Properties by Spray-Drying Process. Electrochimica Acta, 2015, 173, 581-587.	5.2	38
241	Superior Electrochemical Properties of Nanofibers Composed of Hollow CoFe <sub>2</sub> O <sub>4</sub> Nanospheres Covered with Onionâ€Like Graphitic Carbon. Chemistry - A European Journal, 2015, 21, 18202-18208.	3.3	26
242	Synthesis of hollow cobalt oxide nanopowders by a salt-assisted spray pyrolysis process applying nanoscale Kirkendall diffusion and their electrochemical properties. Physical Chemistry Chemical Physics, 2015, 17, 31988-31994.	2.8	11
243	General Formation of Tin Nanoparticles Encapsulated in Hollow Carbon Spheres for Enhanced Lithium Storage Capability. Small, 2015, 11, 2157-2163.	10.0	48
244	Superior electrochemical properties of rutile VO2-carbon composite microspheres as a promising anode material for lithium ion batteries. Electrochimica Acta, 2015, 156, 179-187.	5.2	38
245	Three-dimensional porous graphene-metal oxide composite microspheres: Preparation and application in Li-ion batteries. Nano Research, 2015, 8, 1584-1594.	10.4	74
246	Sodium ion storage properties of WS <sub>2</sub> -decorated three-dimensional reduced graphene oxide microspheres. Nanoscale, 2015, 7, 3965-3970.	5.6	134
247	Fabrication and electrochemical performance of 0.6Li2MnO3-0.4Li(Ni1/3Co1/3Mn1/3)O2 microspheres by two-step spray-drying process. Scientific Reports, 2015, 4, 5752.	3.3	12
248	3D MoS <sub>2</sub> –Graphene Microspheres Consisting of Multiple Nanospheres with Superior Sodium Ion Storage Properties. Advanced Functional Materials, 2015, 25, 1780-1788.	14.9	482
249	Pure and Palladium‣oaded Co <sub>3</sub> O <sub>4</sub> Hollow Hierarchical Nanostructures with Giant and Ultraselective Chemiresistivity to Xylene and Toluene. Chemistry - A European Journal, 2015, 21, 5872-5878.	3.3	52
250	An efficient ribitol-specific dehydrogenase from Enterobacter aerogenes. Enzyme and Microbial Technology, 2015, 72, 56-64.	3.2	6
251	Synergetic compositional and morphological effects for improved Na <sup>+</sup> storage properties of Ni <sub>3</sub> Co <sub>6</sub> S <sub>8</sub> -reduced graphene oxide composite powders. Nanoscale, 2015, 7, 6230-6237.	5.6	57
252	Facile synthesis of multi-shell structured binary metal oxide powders with a Ni/Co mole ratio of 1:2 for Li-lon batteries. Journal of Power Sources, 2015, 284, 481-488.	7.8	31

#	Article	IF	CITATIONS
253	Electrochemical properties of MnS–C and MnO–C composite powders prepared via spray drying process. Journal of Power Sources, 2015, 295, 9-15.	7.8	36
254	Multiphase and Double-Layer NiFe2O4@NiO-Hollow-Nanosphere-Decorated Reduced Graphene Oxide Composite Powders Prepared by Spray Pyrolysis Applying Nanoscale Kirkendall Diffusion. ACS Applied Materials & Interfaces, 2015, 7, 16842-16849.	8.0	57
255	Co9S8–carbon composite as anode materials with improved Na-storage performance. Carbon, 2015, 94, 85-90.	10.3	112
256	Aerosol-assisted rapid synthesis of SnS-C composite microspheres as anode material for Na-ion batteries. Nano Research, 2015, 8, 1595-1603.	10.4	115
257	Capacitive properties of reduced graphene oxide microspheres with uniformly dispersed nickel sulfide nanocrystals prepared by spray pyrolysis. Electrochimica Acta, 2015, 167, 287-293.	5.2	8
258	Two-step spray-drying synthesis of dense and highly luminescent YAC:Ce <sup>3+</sup> phosphor powders with spherical shape. RSC Advances, 2015, 5, 8345-8350.	3.6	18
259	Kilogram-Scale Synthesis of Pd-Loaded Quintuple-Shelled Co <sub>3</sub> O <sub>4</sub> Microreactors and Their Application to Ultrasensitive and Ultraselective Detection of Methylbenzenes. ACS Applied Materials & Interfaces, 2015, 7, 7717-7723.	8.0	56
260	One-pot synthesis of core–shell-structured tin oxide–carbon composite powders by spray pyrolysis for use as anode materials in Li-ion batteries. Carbon, 2015, 88, 262-269.	10.3	34
261	Design and Synthesis of Bubble-Nanorod-Structured Fe <sub>2</sub> O <sub>3</sub> –Carbon Nanofibers as Advanced Anode Material for Li-Ion Batteries. ACS Nano, 2015, 9, 4026-4035.	14.6	426
262	Design and synthesis of micron-sized spherical aggregates composed of hollow Fe <sub>2</sub> O <sub>3</sub> nanospheres for use in lithium-ion batteries. Nanoscale, 2015, 7, 8361-8367.	5.6	65
263	Novel cobalt oxide-nanobubble-decorated reduced graphene oxide sphere with superior electrochemical properties prepared by nanoscale Kirkendall diffusion process. Nano Energy, 2015, 17, 17-26.	16.0	70
264	Synthesis and electrochemical properties of spherical and hollow-structured NiO aggregates created by combining the Kirkendall effect and Ostwald ripening. Nanoscale, 2015, 7, 19620-19626.	5.6	63
265	Synergetic Effect of Yolk–Shell Structure and Uniform Mixing of SnS–MoS <sub>2</sub> Nanocrystals for Improved Na-Ion Storage Capabilities. ACS Applied Materials & Interfaces, 2015, 7, 24694-24702.	8.0	104
266	Perforated Metal Oxide–Carbon Nanotube Composite Microspheres with Enhanced Lithium-Ion Storage Properties. ACS Nano, 2015, 9, 10173-10185.	14.6	91
267	Sodium-ion storage properties of nickel sulfide hollow nanospheres/reduced graphene oxide composite powders prepared by a spray drying process and the nanoscale Kirkendall effect. Nanoscale, 2015, 7, 16781-16788.	5.6	150
268	Synthesis of NiO Nanofibers Composed of Hollow Nanospheres with Controlled Sizes by the Nanoscale Kirkendall Diffusion Process and Their Electrochemical Properties. ACS Applied Materials & Interfaces, 2015, 7, 25641-25647.	8.0	50
269	Modification of Structural and Luminescence Properties of Graphene Quantum Dots by Gamma Irradiation and Their Application in a Photodynamic Therapy. ACS Applied Materials & Interfaces, 2015, 7, 25865-25874.	8.0	94
270	Superior electrochemical properties of α-Fe 2 O 3 nanofibers with a porous core/dense shell structure formed from iron acetylacetonate-polyvinylpyrrolidone composite fibers. Electrochimica Acta, 2015, 154, 211-218.	5.2	13

#	Article	lF	CITATIONS
271	Yolk–shell structured Gd <sub>2</sub> O <sub>3</sub> :Eu <sup>3+</sup> phosphor prepared by spray pyrolysis: the effect of preparation conditions on microstructure and luminescence properties. Physical Chemistry Chemical Physics, 2015, 17, 1325-1331.	2.8	22
272	Superior electrochemical properties of spherical-like Co2(OH)3Cl-reduced graphene oxide composite powders with ultrafine nanocrystals. Carbon, 2015, 84, 14-23.	10.3	23
273	ÂA New Concept for Obtaining SnO <sub>2</sub> Fiberâ€inâ€Tube Nanostructures with Superior Electrochemical Properties. Chemistry - A European Journal, 2015, 21, 371-376.	3.3	61
274	Superior Lithiumâ€lon Storage Properties of Siâ€Based Composite Powders with Unique Si@Carbon@Void@Graphene Configuration. Chemistry - A European Journal, 2015, 21, 2076-2082.	3.3	23
275	Simultaneous pretreatment and saccharification: Green technology for enhanced sugar yields from biomass using a fungal consortium. Bioresource Technology, 2015, 179, 50-57.	9.6	90
276	Formation of core–shell-structured Zn2SnO4–carbon microspheres with superior electrochemical properties by one-pot spray pyrolysis. Nanoscale, 2015, 7, 701-707.	5.6	31
277	Screening and characterization of an Agrobacterium tumefaciens mutant strain producing high level of coenzyme Q10. Process Biochemistry, 2015, 50, 33-39.	3.7	8
278	Ultrasensitive detection of trimethylamine using Rh-doped SnO2 hollow spheres prepared by ultrasonic spray pyrolysis. Sensors and Actuators B: Chemical, 2015, 207, 330-337.	7.8	84
279	Electrochemical properties of cobalt hydroxychloride microspheres as a new anode material for Li-ion batteries. Scientific Reports, 2015, 4, 5785.	3.3	30
280	Flame Spray Pyrolysis for Finding Multicomponent Nanomaterials with Superior Electrochemical Properties in the CoO <sub><i>x</i></sub> â€FeO <sub><i>x</i></sub> System for Use in Lithiumâ€Ion Batteries. Chemistry - an Asian Journal, 2014, 9, 2826-2830.	3.3	5
281	Superior electrochemical performances of double-shelled CuO yolk–shell powders formed from spherical copper nitrate–polyvinylpyrrolidone composite powders. RSC Advances, 2014, 4, 58231-58237.	3.6	6
282	Macroporous Fe <sub>3</sub> O <sub>4</sub> /Carbon Composite Microspheres with a Short Li <sup>+</sup> Diffusion Pathway for the Fast Charge/Discharge of Lithium Ion Batteries. Chemistry - A European Journal, 2014, 20, 11078-11083.	3.3	36
283	Oneâ€Pot Method for Synthesizing Sphericalâ€Like Metal Sulfide–Reduced Graphene Oxide Composite Powders with Superior Electrochemical Properties for Lithiumâ€Ion Batteries. Chemistry - A European Journal, 2014, 20, 12183-12189.	3.3	36
284	Uniform Decoration of Vanadium Oxide Nanocrystals on Reduced Grapheneâ€Oxide Balls by an Aerosol Process for Lithiumâ€Ion Battery Cathode Material. Chemistry - A European Journal, 2014, 20, 6294-6299.	3.3	45
285	Role of a remote leucine residue in the catalytic function of polyol dehydrogenase. Molecular BioSystems, 2014, 10, 3255-3263.	2.9	12
286	Excellent Electrochemical Properties of Yolk–Shell MoO <sub>3</sub> Microspheres Formed by Combustion of Molybdenum Oxide–Carbon Composite Microspheres. Chemistry - an Asian Journal, 2014, 9, 1011-1015.	3.3	27
287	Preparation of Yolkâ€Shell and Filled Co <sub>9</sub> S <sub>8</sub> Microspheres and Comparison of their Electrochemical Properties. Chemistry - an Asian Journal, 2014, 9, 572-576.	3.3	69
288	Electrochemical Properties of Hollowâ€&tructured MnS–Carbon Nanocomposite Powders Prepared by a Oneâ€Pot Spray Pyrolysis Process. Chemistry - an Asian Journal, 2014, 9, 590-595.	3.3	25

#	Article	IF	CITATIONS
289	Synthesis for Yolkâ€shellâ€structured Metal Sulfide Powders with Excellent Electrochemical Performances for Lithiumâ€ion Batteries. Small, 2014, 10, 474-478.	10.0	127
290	Electrochemical properties of ultrafine TiO2-doped MoO3 nanoplates prepared by one-pot flame spray pyrolysis. RSC Advances, 2014, 4, 17382.	3.6	19
291	Enhancement of light-harvesting efficiency of dye-sensitized solar cells via forming TiO2 composite double layers with down/up converting phosphor dispersion. RSC Advances, 2014, 4, 10039.	3.6	28
292	Recent progress in electrode materials produced by spray pyrolysis for next-generation lithium ion batteries. Advanced Powder Technology, 2014, 25, 18-31.	4.1	80
293	Ultraselective and ultrasensitive detection of trimethylamine using MoO3 nanoplates prepared by ultrasonic spray pyrolysis. Sensors and Actuators B: Chemical, 2014, 195, 189-196.	7.8	107
294	Superior electrochemical properties of MoS2 powders with a MoS2@void@MoS2 configuration. Nanoscale, 2014, 6, 4508.	5.6	41
295	Electrochemical properties of bare nickel sulfide and nickel sulfide–carbon composites prepared by one-pot spray pyrolysis as anode materials for lithium secondary batteries. Journal of Power Sources, 2014, 251, 480-487.	7.8	48
296	Ultraselective and ultrasensitive detection of H2S in highly humid atmosphere using CuO-loaded SnO2 hollow spheres for real-time diagnosis of halitosis. Sensors and Actuators B: Chemical, 2014, 194, 371-376.	7.8	164
297	Crumpled Graphene–Molybdenum Oxide Composite Powders: Preparation and Application in Lithiumâ€ion Batteries. ChemSusChem, 2014, 7, 523-528.	6.8	126
298	Design and Fabrication of New Nanostructured SnO <sub>2</sub> â€Carbon Composite Microspheres for Fast and Stable Lithium Storage Performance. Small, 2014, 10, 3240-3245.	10.0	66
299	Preparation of Li <sub>4</sub> Ti <sub>5</sub> O <sub>12</sub> Yolk–Shell Powders by Spray Pyrolysis and their Electrochemical Properties. Chemistry - an Asian Journal, 2014, 9, 443-446.	3.3	23
300	Kilogram‣cale Production of SnO <sub>2</sub> Yolk–Shell Powders by a Sprayâ€Drying Process Using Dextrin as Carbon Source and Drying Additive. Chemistry - A European Journal, 2014, 20, 5835-5839.	3.3	36
301	High performance chemiresistive H <sub>2</sub> S sensors using Ag-loaded SnO <sub>2</sub> yolk–shell nanostructures. RSC Advances, 2014, 4, 16067-16074.	3.6	58
302	Oneâ€Pot Synthesis of Pd‣oaded SnO <sub>2</sub> Yolk–Shell Nanostructures for Ultraselective Methyl Benzene Sensors. Chemistry - A European Journal, 2014, 20, 2737-2741.	3.3	93
303	Effect of esterification reaction of citric acid and ethylene glycol on the formation of multi-shelled cobalt oxide powders with superior electrochemical properties. Nano Research, 2014, 7, 1738-1748.	10.4	47
304	Yolk–shell structured Y2O3:Eu3+ phosphor powders with enhanced photoluminescence properties prepared by spray pyrolysis. CrystEngComm, 2014, 16, 6170.	2.6	13
305	Rh-catalyzed WO <sub>3</sub> with anomalous humidity dependence of gas sensing characteristics. RSC Advances, 2014, 4, 53130-53136.	3.6	79
306	Enhanced Ethanol Sensing Characteristics of In <sub>2</sub> O <sub>3</sub> -Decorated NiO Hollow Nanostructures via Modulation of Hole Accumulation Layers. ACS Applied Materials & Interfaces, 2014, 6, 18197-18204.	8.0	144

#	Article	IF	CITATIONS
307	Comparison of the electrochemical properties of yolk–shell and dense structured CoFe <sub>2</sub> O <sub>4</sub> powders prepared by a spray pyrolysis process. RSC Advances, 2014, 4, 40188.	3.6	13
308	Large scale production of yolk–shell β-tricalcium phosphate powders, and their bioactivities as novel bone substitutes. Physical Chemistry Chemical Physics, 2014, 16, 16962.	2.8	7
309	Large-scale production of spherical Y <sub>2</sub> O <sub>3</sub> :Eu <sup>3+</sup> phosphor powders with narrow size distribution using a two-step spray drying method. RSC Advances, 2014, 4, 62965-62970.	3.6	9
310	Large-scale production of fine-sized Zn2SiO4:Mn phosphor microspheres with a dense structure and good photoluminescence properties by a spray-drying process. RSC Advances, 2014, 4, 43606-43611.	3.6	13
311	Characteristics of precursor powders of a nickel-rich cathode material prepared by a spray drying process using water-soluble metal salts. RSC Advances, 2014, 4, 44203-44207.	3.6	20
312	Electrochemical properties of ultrafine Sb nanocrystals embedded in carbon microspheres for use as Na-ion battery anode materials. Chemical Communications, 2014, 50, 12322-12324.	4.1	130
313	Controllable synthesis of yolk–shell-structured metal oxides with seven to ten components for finding materials with superior lithium storage properties. Nanoscale, 2014, 6, 12421-12425.	5.6	20
314	Using Simple Spray Pyrolysis to Prepare Yolk–Shellâ€&tructured ZnO–Mn <sub>3</sub> O <sub>4</sub> Systems with the Optimum Composition for Superior Electrochemical Properties. Chemistry - A European Journal, 2014, 20, 3014-3018.	3.3	50
315	Superior Supercapacitor Properties of Composite Powders with Amorphous NiO Nanoclusters Distributed Uniformly in an Amorphous Carbon Matrix. Chemistry - an Asian Journal, 2014, 9, 2453-2457.	3.3	9
316	Superior cycling and rate performances of rattle-type CoMoO4 microspheres prepared by one-pot spray pyrolysis. RSC Advances, 2014, 4, 17873.	3.6	28
317	Advanced yolk–shell hydroxyapatite for bone graft materials: kilogram-scale production and structure-in vitro bioactivity relationship. RSC Advances, 2014, 4, 25234.	3.6	8
318	Ultrafast Synthesis of Yolk-Shell and Cubic NiO Nanopowders and Application in Lithium Ion Batteries. ACS Applied Materials & Interfaces, 2014, 6, 2312-2316.	8.0	90
319	Hierarchical MoSe <sub>2</sub> yolk–shell microspheres with superior Na-ion storage properties. Nanoscale, 2014, 6, 10511.	5.6	227
320	Fe3O4-decorated hollow graphene balls prepared by spray pyrolysis process for ultrafast and long cycle-life lithium ion batteries. Carbon, 2014, 79, 58-66.	10.3	71
321	Electrochemical properties of yolk-shell structured layered-layered composite cathode powders prepared by spray pyrolysis. Electrochimica Acta, 2014, 144, 288-294.	5.2	8
322	Electrochemical properties of graphene-MnO composite and hollow-structured MnO powders prepared by a simple one-pot spray pyrolysis process. Electrochimica Acta, 2014, 132, 441-447.	5.2	38
323	Study of Co3O4 mesoporous nanosheets prepared by a simple spray-drying process and their electrochemical properties as anode material for lithium secondary batteries. Electrochimica Acta, 2014, 116, 44-50.	5.2	33
324	Cloning and characterization of a galactitol 2-dehydrogenase from Rhizobium legumenosarum and its application in d-tagatose production. Enzyme and Microbial Technology, 2014, 58-59, 44-51.	3.2	26

#	Article	IF	CITATIONS
325	Electrochemical properties of micron-sized, spherical, meso- and macro-porous Co3O4 and CoO–carbon composite powders prepared by a two-step spray drying process. Nanoscale, 2014, 6, 4789.	5.6	36
326	Structureâ€based studies on the metal binding of twoâ€metalâ€dependent sugar isomerases. FEBS Journal, 2014, 281, 3446-3459.	4.7	12
327	Electrochemical properties of cobalt sulfide-carbon composite powders prepared by simple sulfidation process of spray-dried precursor powders. Electrochimica Acta, 2014, 137, 336-343.	5.2	24
328	Electrochemical Properties of Tin Oxide Flake/Reduced Graphene Oxide/Carbon Composite Powders as Anode Materials for Lithiumâ€Ion Batteries. Chemistry - A European Journal, 2014, 20, 15203-15207.	3.3	20
329	Electrochemical properties of tungsten sulfide–carbon composite microspheres prepared by spray pyrolysis. Scientific Reports, 2014, 4, 5755.	3.3	42
330	Rapid continuous synthesis of spherical reduced graphene ball-nickel oxide composite for lithium ion batteries. Scientific Reports, 2014, 4, 5786.	3.3	35
331	One-pot synthesis of manganese oxide-carbon composite microspheres with three dimensional channels for Li-ion batteries. Scientific Reports, 2014, 4, 5751.	3.3	37
332	Electrochemical properties of yolk-shell structured ZnFe2O4 powders prepared by a simple spray drying process as anode material for lithium-ion battery. Scientific Reports, 2014, 4, 5857.	3.3	88
333	Reduction in Acute Ecotoxicity of Paper Mill Effluent by Sequential Application of Xylanase and Laccase. PLoS ONE, 2014, 9, e102581.	2.5	23
334	A new strategy for synthesizing yolk–shell V2O5 powders with low melting temperature for high performance Li-ion batteries. Nanoscale, 2013, 5, 8899.	5.6	60
335	Electrochemical properties of yolk–shell and hollow CoMn2O4 powders directly prepared by continuous spray pyrolysis as negative electrode materials for lithium ion batteries. RSC Advances, 2013, 3, 13110.	3.6	54
336	Yolk–Shell, Hollow, and Singleâ€Crystalline ZnCo <sub>2</sub> O <sub>4</sub> Powders: Preparation Using a Simple Oneâ€Pot Process and Application in Lithiumâ€Ion Batteries. ChemSusChem, 2013, 6, 2111-2116.	6.8	133
337	One-pot facile synthesis of Janus-structured SnO2–CuO composite nanorods and their application as anode materials in Li-ion batteries. Nanoscale, 2013, 5, 4662.	5.6	52
338	Characterization of a novel xylanase from Armillaria gemina and its immobilization onto SiO2 nanoparticles. Applied Microbiology and Biotechnology, 2013, 97, 1081-1091.	3.6	30
339	Electrochemical Properties of Yolk‧hell, Hollow, and Dense WO <sub>3</sub> Particles Prepared by using Spray Pyrolysis. ChemSusChem, 2013, 6, 1320-1325.	6.8	41
340	Morphologies and electrochemical properties ofÂ0.6Li2MnO3·0.4LiCoO2 composite cathode powders prepared byÂspray pyrolysis. Materials Chemistry and Physics, 2013, 142, 438-444.	4.0	4
341	Effects of ratios of Li2MnO3 and Li(Ni1/3Mn1/3Co1/3)O2 phases on the properties of composite cathode powders in spray pyrolysis. Electrochimica Acta, 2013, 103, 110-118.	5.2	39
342	Preparation and electrochemical properties of glass-modified LiCoO2 cathode powders. Journal of Power Sources, 2013, 244, 129-135.	7.8	22

#	Article	IF	CITATIONS
343	Nano-sized LiNi0.5Mn1.5O4 cathode powders with good electrochemical properties prepared by high temperature flame spray pyrolysis. Journal of Industrial and Engineering Chemistry, 2013, 19, 1204-1208.	5.8	11
344	One-Pot Facile Synthesis of Ant-Cave-Structured Metal Oxide–Carbon Microballs by Continuous Process for Use as Anode Materials in Li-Ion Batteries. Nano Letters, 2013, 13, 5462-5466.	9.1	151
345	One-pot rapid synthesis of core–shell structured NiO@TiO2 nanopowders and their excellent electrochemical properties as anode materials for lithium ion batteries. Nanoscale, 2013, 5, 12645.	5.6	41
346	Enzymatic hydrolysis of aspen biomass into fermentable sugars by using lignocellulases from Armillaria gemina. Bioresource Technology, 2013, 133, 307-314.	9.6	32
347	Characteristics of Li2TiO3–LiCrO2 composite cathode powders prepared by ultrasonic spray pyrolysis. Journal of Power Sources, 2013, 244, 336-343.	7.8	14
348	One-pot synthesis of Fe2O3 yolk–shell particles with two, three, and four shells for application as an	5.6	65
349	Yolk–shelled cathode materials with extremely high electrochemical performances prepared by spray pyrolysis. Nanoscale, 2013, 5, 7867.	5.6	58
350	Superior electrochemical properties of LiMn2O4 yolk–shell powders prepared by a simple spray pyrolysis process. Chemical Communications, 2013, 49, 5978.	4.1	55
351	Facile one-pot synthesis of spherical zinc sulfide–carbon nanocomposite powders with superior electrochemical properties as anode materials for Li-ion batteries. Physical Chemistry Chemical Physics, 2013, 15, 16437.	2.8	32
352	Continuous one-pot synthesis of sandwich structured core–shell particles and transformation to yolk–shell particles. Chemical Communications, 2013, 49, 3884.	4.1	9
353	Highly selective and sensitive detection of trimethylamine using WO3 hollow spheres prepared by ultrasonic spray pyrolysis. Sensors and Actuators B: Chemical, 2013, 176, 971-977.	7.8	107
354	Electrochemical properties of nanometer-sized 0.6Li2MnO3·0.4LiNi0.5Mn0.5O2 composite powders prepared by flame spray pyrolysis. Ceramics International, 2013, 39, 331-336.	4.8	12
355	Core–shell-structure Ag–BaTiO3 composite nanopowders prepared directly by flame spray pyrolysis. Materials Chemistry and Physics, 2013, 140, 266-272.	4.0	4
356	Characteristics of stabilized spinel cathode powders obtained by in-situ coating method. Journal of Power Sources, 2013, 244, 625-630.	7.8	9
357	Microbial consortia for saccharification of woody biomass and ethanol fermentation. Fuel, 2013, 107, 815-822.	6.4	90
358	Electrochemical Properties of ZrO2-Doped V2O5 Amorphous Powders with Spherical Shape and Fine Size. ACS Applied Materials & Interfaces, 2013, 5, 3234-3240.	8.0	25
359	Oneâ€Pot Facile Synthesis of Doubleâ€Shelled SnO <sub>2</sub> Yolkâ€Shellâ€Structured Powders by Continuous Process as Anode Materials for Liâ€ion Batteries. Advanced Materials, 2013, 25, 2279-2283.	21.0	378
360	Molecular cloning and characterization of a GH11 endoxylanase from Chaetomium globosum, and its use in enzymatic pretreatment of biomass. Applied Microbiology and Biotechnology, 2013, 97, 7205-7214.	3.6	21

#	Article	IF	CITATIONS
361	Superior electrochemical properties of Co3O4 yolk–shell powders with a filled core and multishells prepared by a one-pot spray pyrolysis. Chemical Communications, 2013, 49, 5678.	4.1	59
362	Oneâ€Pot Synthesis of Yolk–Shell Materials with Single, Binary, Ternary, Quaternary, and Quinary Systems. Small, 2013, 9, 2224-2227.	10.0	54
363	Characterization of a $\hat{1}^2$ -1,4-glucosidase from a newly isolated strain of Pholiota adiposa and its application to the hydrolysis of biomass. Biomass and Bioenergy, 2013, 54, 181-190.	5.7	35
364	Nano-sized Ag–BaTiO3 composite powders with various amount of Ag prepared by spray pyrolysis. Journal of the European Ceramic Society, 2013, 33, 1335-1341.	5.7	10
365	Batteries: Oneâ€Pot Facile Synthesis of Doubleâ€Shelled SnO <sub>2</sub> Yolkâ€Shellâ€Structured Powders by Continuous Process as Anode Materials for Liâ€ion Batteries (Adv. Mater. 16/2013). Advanced Materials, 2013, 25, 2250-2250.	21.0	8
366	Yolk-Shell Materials: One-Pot Synthesis of Yolk-Shell Materials with Single, Binary, Ternary, Quaternary, and Quinary Systems (Small 13/2013). Small, 2013, 9, 2223-2223.	10.0	0
367	Electrochemical Properties of Yolk–Shellâ€&tructured CuO–Fe <sub>2</sub> O <sub>3</sub> Powders with Various Cu/Fe Molar Ratios Prepared by Oneâ€Pot Spray Pyrolysis. ChemSusChem, 2013, 6, 2299-2303.	6.8	20
368	Excellent Electrochemical Properties of Yolk–Shell LiV <sub>3</sub> O <sub>8</sub> Powder and Its Potential as Cathodic Material for Lithiumâ€ion Batteries. Chemistry - A European Journal, 2013, 19, 17305-17309.	3.3	20
369	Electro-Deoxidation Behavior of Graphite Oxide in Aqueous Solution. Journal of Chemical Engineering of Japan, 2013, 46, 245-249.	0.6	1
370	Electrochemical Carbon Formation from a Graphite Anode in Li2O/LiCl Molten Salt. Asian Journal of Chemistry, 2013, 25, 7019-7022.	0.3	7
371	Optimization of Î <sup>2</sup> -Glucosidase Production by a Strain of Stereum hirsutum and Its Application in Enzymatic Saccharification. Journal of Microbiology and Biotechnology, 2013, 23, 351-356.	2.1	9
372	Molecular Determinants of the Cofactor Specificity of Ribitol Dehydrogenase, a Short-Chain Dehydrogenase/Reductase. Applied and Environmental Microbiology, 2012, 78, 3079-3086.	3.1	21
373	Characteristics of BaTiO3-coated Ag powders directly prepared by spray pyrolysis. Journal of the Ceramic Society of Japan, 2012, 120, 15-20.	1.1	1
374	Sintering characteristics of nano-sized Ag–Pd–glass composite powders with high Pd content. Journal of Materials Science, 2012, 47, 7090-7098.	3.7	1
375	Properties of Bi-based glass powders with low glass transition temperature, spherical shape and fine size as the additive of silver conducting paste. Electronic Materials Letters, 2012, 8, 643-648.	2.2	4
376	Combustion characteristics of the heat pellet prepared from the Fe powders obtained by spray pyrolysis. Advanced Powder Technology, 2012, 23, 387-392.	4.1	4
377	Saccharification of poplar biomass by using lignocellulases from Pholiota adiposa. Bioresource Technology, 2012, 120, 264-272.	9.6	18
378	Effects of post-annealing on electrical properties of amorphous Ga-doped Zn–Sn–O semiconductor films. Journal of Non-Crystalline Solids, 2012, 358, 2616-2619.	3.1	4

#	Article	IF	CITATIONS
379	Effect of boric acid on the properties of Li2MnO3·LiNi0.5Mn0.5O2 composite cathode powders prepared by large-scale spray pyrolysis with droplet classifier. Materials Research Bulletin, 2012, 47, 4359-4364.	5.2	13
380	Fine-sized Tb3Al5O12:Ce phosphor powders prepared by spray pyrolysis from spray solution with ethylenediaminetetraacetic acid. Electronic Materials Letters, 2012, 8, 283-287.	2.2	5
381	Characteristics of Fe powders prepared by spray pyrolysis from a spray solution with ethylene glycol as the source material of heat pellet. Metals and Materials International, 2012, 18, 445-449.	3.4	0
382	Immobilization of Pholiota adiposa xylanase onto SiO2 nanoparticles and its application for production of xylooligosaccharides. Biotechnology Letters, 2012, 34, 1307-1313.	2.2	23
383	Characteristics of Ag-doped BaTiO3 nanopowders prepared by spray pyrolysis. Ceramics International, 2012, 38, 2071-2077.	4.8	2
384	Dielectric properties of nano-sized Ba0.7Sr0.3TiO3 powders prepared by spray pyrolysis. Ceramics International, 2012, 38, 4029-4033.	4.8	8
385	Electrochemical properties of nanosized LiCrO2·Li2MnO3 composite powders prepared by a new concept spray pyrolysis. Electrochimica Acta, 2012, 69, 345-350.	5.2	14
386	Characterization of H2O-forming NADH oxidase from Streptococcus pyogenes and its application in l-rare sugar production. Bioorganic and Medicinal Chemistry Letters, 2012, 22, 1931-1935.	2.2	44
387	Synthesis and electrochemical properties of nanorod-shaped LiMn1.5Ni0.5O4 cathode materials for lithium-ion batteries. Materials Chemistry and Physics, 2012, 132, 223-227.	4.0	9
388	Electrochemical properties of nano-sized LiNi1/3Co1/3Mn1/3O2 powders in the range from 56 to 101 nm prepared by flame spray pyrolysis. Materials Chemistry and Physics, 2012, 134, 254-259.	4.0	23
389	Green light-emitting Lu3Al5O12:Ce phosphor powders prepared by spray pyrolysis. Materials Research Bulletin, 2012, 47, 1428-1431.	5.2	29
390	Electrochemical properties of 0.3Li2MnO3·0.7LiNi0.5Mn0.5O2 composite cathode powders prepared by large-scale spray pyrolysis. Materials Research Bulletin, 2012, 47, 2022-2026.	5.2	15
391	Electrochemical properties of Li2O–2B2O3 glass-modified LiMn2O4 powders prepared by spray pyrolysis process. Journal of Power Sources, 2012, 210, 110-115.	7.8	25
392	Electrochemical properties of spherically shaped dense V2O5 cathode powders prepared directly by spray pyrolysis. Journal of Power Sources, 2012, 211, 84-91.	7.8	20
393	Ultrasensitive and selective C2H5OH sensors using Rh-loaded In2O3 hollow spheres. Journal of Materials Chemistry, 2011, 21, 18560.	6.7	103
394	Pb-free glass frits prepared by spray pyrolysis as inorganic binders of Al electrodes in Si solar cells. Journal of Alloys and Compounds, 2011, 509, 6325-6331.	5.5	25
395	Characteristics of ZnO–B2O3–SiO2–CaO glass frits prepared by spray pyrolysis as inorganic binder for Cu electrode. Journal of Alloys and Compounds, 2011, 509, 8077-8081.	5.5	11
396	Characteristics of BaO–B2O3–SiO2 nano glass powders prepared by flame spray pyrolysis as the sintering agent of BaTiO3 ceramics. Journal of Alloys and Compounds, 2011, 509, 7979-7984.	5.5	9

#	Article	IF	CITATIONS
397	Characteristics of nano-sized Ag-Pd (70-30)-glass composite powders prepared by flame spray pyrolysis. Journal of the Ceramic Society of Japan, 2011, 119, 23-28.	1.1	1
398	Properties of La0.8Sr0.2Ga0.8Mg0.2O2.8 electrolyte formed from the nano-sized powders prepared by spray pyrolysis. Journal of the Ceramic Society of Japan, 2011, 119, 752-756.	1.1	0
399	Size-controlled glass frits with spherical shape for Al electrodes in Si solar cells. Journal of the Ceramic Society of Japan, 2011, 119, 954-960.	1.1	1
400	Effect of preparation temperature on the morphology, crystal structure and electrochemical properties of LiV3O8 powders prepared by spray pyrolysis. Materials Chemistry and Physics, 2011, 126, 133-137.	4.0	11
401	Electrochemical properties of nano-sized Li3V2(PO4)3/C composite powders prepared by spray pyrolysis from spray solution with chelating agent. Materials Chemistry and Physics, 2011, 131, 292-296.	4.0	23
402	Low-temperature sintering characteristics of nano-sized BaNd2Ti5O14 and Bi2O3–B2O3–ZnO–SiO2 glass powders prepared by gas-phase reactions. Materials Research Bulletin, 2011, 46, 2112-2116.	5.2	3
403	Air-stable silver-coated copper particles of sub-micrometer size. Journal of Colloid and Interface Science, 2011, 364, 574-581.	9.4	45
404	Low-temperature sintering and electrical properties of strontium- and magnesium-doped lanthanum gallate with V2O5 additive. Journal of Power Sources, 2011, 196, 2971-2978.	7.8	11
405	Characteristics of Li3V2(PO4)3/C powders prepared by ultrasonic spray pyrolysis. Journal of Power Sources, 2011, 196, 6682-6687.	7.8	73
406	Characteristics of nanosized Bi-based glass powders prepared by flame spray pyrolysis as transparent dielectric layer material. Ceramics International, 2011, 37, 687-690.	4.8	2
407	Size-controlled silver-glass composite powders with nanometer size prepared by flame spray pyrolysis. Powder Technology, 2011, 207, 362-369.	4.2	9
408	Effects of precursors of glass material on the characteristics of silver-glass composite powders prepared by spray pyrolysis. Metals and Materials International, 2011, 17, 315-319.	3.4	0
409	Preparation of nanometer AlN powders by combining spray pyrolysis with carbothermal reduction and nitridation. Ceramics International, 2011, 37, 1967-1971.	4.8	18
410	Characteristics of Eu2+-doped Ca-α-SiAlON phosphor powders prepared by spray pyrolysis process. Optical Materials, 2011, 33, 538-542.	3.6	8
411	Nanosized LiMn2O4 powders prepared by flame spray pyrolysis from aqueous solution. Journal of Power Sources, 2011, 196, 2858-2862.	7.8	23
412	Characteristics of Ag–Pd–glass composite and Ag–Pd alloy powders prepared by spray pyrolysis. Powder Technology, 2011, 207, 318-323.	4.2	0
413	Enhanced C2H5OH sensing characteristics of nano-porous In2O3 hollow spheres prepared by sucrose-mediated hydrothermal reaction. Sensors and Actuators B: Chemical, 2011, 155, 512-518.	7.8	89
414	Characteristics of Pb-based glass powders prepared by spray pyrolysis as inorganic additive of Al paste for solar cell. Solar Energy Materials and Solar Cells, 2011, 95, 34-38.	6.2	4

#	Article	IF	CITATIONS
415	Design of Selective Gas Sensors Using Additive-Loaded In2O3 Hollow Spheres Prepared by Combinatorial Hydrothermal Reactions. Sensors, 2011, 11, 10603-10614.	3.8	46
416	Preparation of silver-glass composite powder and conducting film. Journal of the Ceramic Society of Japan, 2010, 118, 353-356.	1.1	2
417	Effect of preparation conditions on the properties of silver-glass composite powders prepared by spray pyrolysis. Journal of the Ceramic Society of Japan, 2010, 118, 25-29.	1.1	2
418	Properties of nano-sized glass powders prepared by flame spray pyrolysis as an inorganic binder in ink-jet printing. Journal of the Ceramic Society of Japan, 2010, 118, 613-616.	1.1	2
419	BaMgAl10O17: Eu2+ phosphor powders prepared from precursor powders with a hollow and thin wall structure containing NH4F flux. Electronic Materials Letters, 2010, 6, 81-86.	2.2	6
420	Eu-doped B2O3–ZnO–PbO glass phosphor powders withÂspherical shape and fine size prepared by spray pyrolysis. Applied Physics A: Materials Science and Processing, 2010, 98, 671-677.	2.3	2
421	Characteristics of BaNd2Ti5O14 powders directly prepared by high-temperature spray pyrolysis. Ceramics International, 2010, 36, 63-68.	4.8	2
422	Characteristics of samaria-doped ceria nanoparticles prepared by spray pyrolysis. Ceramics International, 2010, 36, 465-471.	4.8	15
423	Effect of precursor types on the characteristics of the Pb-based glass powders prepared by spray pyrolysis. Ceramics International, 2010, 36, 395-399.	4.8	1
424	Firing characteristics of size-controlled silver–glass composite powders prepared by spray pyrolysis. Powder Technology, 2010, 198, 347-353.	4.2	5
425	Electrochemical properties of LiNi0.8Co0.2â~'xAlxO2 (0≤â‰0.1) cathode particles prepared by spray pyrolysis from the spray solutions with and without organic additives. Metals and Materials International, 2010, 16, 299-303.	3.4	38
426	Characteristics of fine size Fe-Ni alloy powders directly prepared by spray pyrolysis. Metals and Materials International, 2010, 16, 643-647.	3.4	8
427	Characteristics of Fe powders prepared by spray pyrolysis from various types of Fe precursors as a heat pellet material. Metals and Materials International, 2010, 16, 941-946.	3.4	7
428	Design of particles by spray pyrolysis and recent progress in its application. Korean Journal of Chemical Engineering, 2010, 27, 1621-1645.	2.7	137
429	Synthesis of nano-sized biphasic calcium phosphate ceramics with spherical shape by flame spray pyrolysis. Journal of Materials Science: Materials in Medicine, 2010, 21, 1143-1149.	3.6	41
430	Conductive silver films formed from nano-sized silver powders prepared by flame spray pyrolysis. Materials Chemistry and Physics, 2010, 124, 959-963.	4.0	10
431	Electrical and morphological properties of conducting layers formed from the silver–glass composite conducting powders prepared by spray pyrolysis. Journal of Colloid and Interface Science, 2010, 343, 1-6.	9.4	6
432	Effect of oxide additives on the sintering behavior and electrical properties of strontium- and magnesium-doped lanthanum gallate. Journal of the European Ceramic Society, 2010, 30, 2593-2601.	5.7	14

#	Article	IF	CITATIONS
433	Effects of drying control chemical additive on properties of Li4Ti5O12 negative powders prepared by spray pyrolysis. Journal of Power Sources, 2010, 195, 4327-4331.	7.8	23
434	Luminescence comparison of YAG:Ce phosphors prepared by microwave heating and precipitation methods. Physica B: Condensed Matter, 2010, 405, 1615-1618.	2.7	24
435	Morphological and electrochemical properties of LiV3O8 cathode powders prepared by spray pyrolysis. Electrochimica Acta, 2010, 55, 6088-6092.	5.2	45
436	Design of selective gas sensors using electrospun Pd-doped SnO2 hollow nanofibers. Sensors and Actuators B: Chemical, 2010, 150, 191-199.	7.8	227
437	Effect of BaF2 as the source of Ba component and flux material in the preparation of Ba1.1Sr0.88SiO4:Eu0.02 phosphor by spray pyrolysis. Ceramics International, 2010, 36, 339-343.	4.8	5
438	Characteristics of Y3Al5O12:Ce phosphor powders prepared by spray pyrolysis from ethylenediaminetetraacetic acid solution. Ceramics International, 2010, 36, 611-615.	4.8	41
439	Size-controlled Bi-based glass powders prepared by spray pyrolysis as inorganic additives for silver electrode. Ceramics International, 2010, 36, 1171-1176.	4.8	4
440	Characteristics of $\hat{I}\pm\hat{a}\in^2$ - and $\hat{I}^2$ -Sr2SiO4:Eu2+ phosphor powders prepared by spray pyrolysis. Ceramics International, 2010, 36, 1233-1238.	4.8	26
441	Characteristics of Bi-based glass powders with various glass transition temperatures prepared by spray pyrolysis. Ceramics International, 2010, 36, 1749-1753.	4.8	3
442	Characteristics of Ag powders coated with Pb-based glass material prepared by spray pyrolysis under various gas environments. Ceramics International, 2010, 36, 2477-2483.	4.8	3
443	Composite conducting powders with core–shell structure as the new concept of electrode material. Colloids and Surfaces A: Physicochemical and Engineering Aspects, 2010, 360, 69-73.	4.7	2
444	Nano-sized silver powders coated with Pb-based glass material with high glass transition temperature. Colloids and Surfaces A: Physicochemical and Engineering Aspects, 2010, 361, 45-50.	4.7	5
445	SiO[sub 2]-Tolerant Grain-Boundary Conduction in Sr- and Mg-Doped Lanthanum Gallate. Electrochemical and Solid-State Letters, 2010, 13, B28.	2.2	6
446	Characteristics of nano-sized silver–glass composite powders prepared by flame spray pyrolysis. Journal of Alloys and Compounds, 2010, 489, 456-460.	5.5	7
447	Fine size Pb-based glass frit with spherical shape as the inorganic binder of Al electrode for Si solar cells. Journal of Alloys and Compounds, 2010, 490, 488-492.	5.5	21
448	Characteristics of Pb-based glass frit prepared by spray pyrolysis as the inorganic binder of silver electrode for Si solar cells. Journal of Alloys and Compounds, 2010, 490, 582-588.	5.5	16
449	Characteristics of silver–glass composite powders as the silver electrode for Si solar cells. Journal of Alloys and Compounds, 2010, 491, 584-588.	5.5	14
450	Effect of gas environment on the properties of silver–glass composite powders with core–shell structure prepared by spray pyrolysis. Journal of Alloys and Compounds, 2010, 492, 723-730.	5.5	2

#	Article	IF	CITATIONS
451	Effect of preparation conditions and types of spray solutions on the formation of nano-sized silver–glass composite powders in flame spray pyrolysis. Journal of Alloys and Compounds, 2010, 496, 536-542.	5.5	1
452	Characteristics of Bi-based glass frit having similar mean size and morphology to those of silver powders at high firing temperatures. Journal of Alloys and Compounds, 2010, 497, 259-266.	5.5	28
453	Characteristics of the glass powders with low Pb content directly prepared by spray pyrolysis. Journal of Alloys and Compounds, 2010, 502, 158-162.	5.5	2
454	Effects of types of drying control chemical additives on the morphologies and electrochemical properties of Li4Ti5O12 anode powders prepared by spray pyrolysis. Journal of Alloys and Compounds, 2010, 506, 913-916.	5.5	19
455	Fine size (Y,Gd)BO3:Eu phosphor powders prepared from precursor powders with hollow shape and large size. Journal of Alloys and Compounds, 2010, 503, 260-265.	5.5	6
456	Synthesis and Electrochemical Characterization of Polypyrrole/Multi-walled Carbon Nanotube Composite Electrodes for Supercapacitor Applications. Bulletin of the Korean Chemical Society, 2010, 31, 1228-1232.	1.9	47
457	Characteristics of Silver Electrode Formed from Nano-Sized Silver and Glass powders. Journal of Korean Institute of Metals and Materials, 2010, 48, .	1.0	0
458	The Role of Carbon Black in the Preparation of GdPO <sub>4</sub> :Tb Phosphor Powders by Spray Pyrolysis. Japanese Journal of Applied Physics, 2009, 48, 116503.	1.5	2
459	The effects of glass powders prepared by spray pyrolysis on the structures and conductivities of silver electrode. Materials Chemistry and Physics, 2009, 118, 25-31.	4.0	6
460	Nanosized barium ferrite powders prepared by spray pyrolysis from citric acid solution. Ceramics International, 2009, 35, 1933-1937.	4.8	19
461	Synthesis of spherical shape borate-based bioactive glass powders prepared by ultrasonic spray pyrolysis. Ceramics International, 2009, 35, 2103-2109.	4.8	16
462	Characteristics of spherical-shaped Li4Ti5O12 anode powders prepared by spray pyrolysis. Journal of Physics and Chemistry of Solids, 2009, 70, 40-44.	4.0	41
463	Effects of preparation conditions on the electrochemical and morphological characteristics of Li4Ti5O12 powders prepared by spray pyrolysis. Journal of Power Sources, 2009, 189, 185-190.	7.8	47
464	Electrochemical properties of Cu6Sn5 alloy powders directly prepared by spray pyrolysis. Journal of Power Sources, 2009, 189, 163-168.	7.8	34
465	Size control of Pb-based glass powders between 38 and 84 nm in the flame spray pyrolysis. Journal of Electroceramics, 2009, 23, 236-241.	2.0	2
466	Spherical shape Ba-based glass powders prepared by spray pyrolysis for MLCCs. Journal of Electroceramics, 2009, 23, 437-441.	2.0	3
467	Effects of La content on the properties of Ba1â^'xLaxTiO3 powders prepared by spray pyrolysis. Metals and Materials International, 2009, 15, 809-814.	3.4	12
468	Preparation and characteristics ofÂaÂBaO–Al2O3–B2O3–SiO2–La2O3 glass ceramic via spray pyrolysis. Applied Physics A: Materials Science and Processing, 2009, 94, 411-417.	2.3	2

#	Article	IF	CITATIONS
469	Nano-sized α and β-TCP powders prepared by high temperature flame spray pyrolysis. Materials Science and Engineering C, 2009, 29, 1288-1292.	7.3	19
470	Preparation of LSGM powders for low temperature sintering. Solid State Ionics, 2009, 180, 788-791.	2.7	24
471	Luminescence enhancement of Eu-doped calcium magnesium silicate blue phosphor for UV-LED application. Journal of Luminescence, 2009, 129, 615-619.	3.1	41
472	Effects of BaF2 flux on the properties of yellow-light-emitting terbium aluminum garnet phosphor powders prepared by spray pyrolysis. Optical Materials, 2009, 31, 870-875.	3.6	27
473	Effects of precursor types of Fe and Ni components on the properties of NiFe2O4 powders prepared by spray pyrolysis. Journal of Magnetism and Magnetic Materials, 2009, 321, 619-623.	2.3	35
474	The characteristics of Ni–Co–Mn–O precursor and Li(Ni1/3Co1/3Mn1/3)O2 cathode powders prepared by spray pyrolysis. Ceramics International, 2009, 35, 1205-1210.	4.8	20
475	Fine-sized LiNi0.8Co0.15Mn0.05O2 cathode particles prepared by spray pyrolysis from the polymeric precursor solutions. Ceramics International, 2009, 35, 1633-1639.	4.8	19
476	Sintering behavior of La2O3–B2O3–TiO2 glass powders prepared by spray pyrolysis for low temperature co-fired ceramics. Ceramics International, 2009, 35, 1829-1835.	4.8	5
477	Fine-sized BaMgAl10O17:Eu2+ phosphor powders prepared by spray pyrolysis from the spray solution with BaF2 flux. Ceramics International, 2009, 35, 2651-2657.	4.8	10
478	Effects of the ratio of manganese and nickel components on the characteristics of Lix(MnyNi1â^'y)Oz cathode powders prepared by spray pyrolysis. Journal of Alloys and Compounds, 2009, 469, 304-309.	5.5	4
479	Characteristics of Ce0.6Tb0.4MgAl11O19 phosphor powders prepared by high temperature flame spray pyrolysis. Journal of Alloys and Compounds, 2009, 472, 367-372.	5.5	1
480	Fine-sized Y3Al5O12:Ce phosphor powders prepared by spray pyrolysis from the spray solution with barium fluoride flux. Journal of Alloys and Compounds, 2009, 477, 776-779.	5.5	63
481	Spherical shape Ni–Co alloy powders directly prepared by spray pyrolysis. Journal of Alloys and Compounds, 2009, 478, 206-209.	5.5	9
482	Characteristics of Sn–Ni alloy powders directly prepared by spray pyrolysis. Journal of Alloys and Compounds, 2009, 478, 177-180.	5.5	10
483	Firing characteristics of La0.8Sr0.2Ga0.8Mg0.2O3â^î´ electrolyte powders prepared by spray pyrolysis. Journal of Alloys and Compounds, 2009, 487, 693-697.	5.5	11
484	Characteristics of size controlled hydroxyapatite powders with nanometer size prepared by flame spray pyrolysis. Journal of the Ceramic Society of Japan, 2009, 117, 1060-1064.	1.1	3
485	Synthesis and characterization of NiFe2O4 nanopowders via spray pyrolysis. Journal of the Ceramic Society of Japan, 2009, 117, 1069-1073.	1.1	4
486	Characteristics of carbon-glass composite powders with spherical shape and submicron size prepared by spray pyrolysis from colloidal spray solution. Journal of the Ceramic Society of Japan, 2009, 117, 1277-1280.	1.1	0

#	Article	IF	CITATIONS
487	Properties of lithium cobaltate powders prepared by FEAG and ultrasonic spray pyrolysis process. Journal of the Ceramic Society of Japan, 2009, 117, 709-712.	1.1	1
488	Characteristics of nano-sized tin dioxide powders prepared by spray pyrolysis. Journal of the Ceramic Society of Japan, 2009, 117, 922-925.	1,1	5
489	Properties of Li2O-ZnO-Al2O3-SiO2 glass-ceramic system prepared by spray pyrolysis. Journal of the Ceramic Society of Japan, 2009, 117, 407-410.	1.1	0
490	Effect of glass powders with spherical shape and fine size on the sintering behavior and dielectric properties of BaTiO3 ceramics. Journal of the Ceramic Society of Japan, 2009, 117, 675-679.	1.1	2
491	Properties of Li2O-ZnO-Al2O3-SiO2 glass-ceramic system prepared by spray pyrolysis. Journal of the Ceramic Society of Japan, 2009, 117, 717.	1.1	0
492	Firing characteristics of nano-sized glass powders prepared by flame spray pyrolysis for electrode application. Journal of the Ceramic Society of Japan, 2009, 117, 1311-1316.	1.1	7
493	Effect of alkali metal on the properties of Bi-based glass powders prepared by spray pyrolysis. Applied Physics A: Materials Science and Processing, 2008, 90, 733-737.	2.3	5
494	Gd2O3:Eu phosphor powders prepared using a size-controllable droplet generator. Optical Materials, 2008, 30, 1810-1815.	3.6	3
495	Fine-sized LiNi0.8Co0.15Mn0.05O2 cathode powders prepared by combined process of gas-phase reaction and solid-state reaction methods. Journal of Power Sources, 2008, 178, 387-392.	7.8	31
496	Nano-sized barium titanate powders with tetragonal crystal structure prepared by flame spray pyrolysis. Journal of the European Ceramic Society, 2008, 28, 109-115.	5.7	21
497	Droplet size control in the filter expansion aerosol generator. Journal of the European Ceramic Society, 2008, 28, 2617-2623.	5.7	5
498	DMF effect on the morphology and the luminescence properties of Y2O3:Eu3+ red phosphor prepared by spray pyrolysis. Journal of Industrial and Engineering Chemistry, 2008, 14, 224-229.	5.8	22
499	LiFePO4/C cathode powders prepared by spray pyrolysis from the colloidal spray solution containing nano-sized carbon black. Materials Chemistry and Physics, 2008, 107, 328-333.	4.0	51
500	LiCo1â^'xAlxO2 (0≤â‰ੳ.05) cathode powders prepared from the nanosized Co1â^'xAlxOy precursor powders. Materials Chemistry and Physics, 2008, 112, 536-541.	4.0	16
501	Nano-sized manganese oxide particles prepared by low-pressure spray pyrolysis using FEAG process. Materials Research Bulletin, 2008, 43, 590-600.	5.2	8
502	Morphologies and crystal structures of nano-sized Ba1â^'xSrxTiO3 primary particles prepared by flame spray pyrolysis. Materials Research Bulletin, 2008, 43, 1789-1799.	5.2	16
503	Characteristics of ZnO–B2O3–CaO–Na2O–P2O5 glass powders prepared by spray pyrolysis. Journal of Non-Crystalline Solids, 2008, 354, 3012-3018.	3.1	9
504	The characteristics of Li(CoxNi1â^'x)O2 cathode powders formed from the fine-sized Co3O4/NiO precursor powders. Journal of Alloys and Compounds, 2008, 450, 457-462.	5.5	4

#	Article	IF	CITATIONS
505	Eu-doped Ca8Mg(SiO4)4Cl2 phosphor particles prepared by spray pyrolysis from the colloidal spray solution containing ammonium chloride. Journal of Alloys and Compounds, 2008, 457, 429-434.	5.5	24
506	Nano-sized hydroxyapatite powders prepared by flame spray pyrolysis. Journal of Alloys and Compounds, 2008, 464, 282-287.	5.5	75
507	Ca7.97-xMg(SiO4)4Cl2:Eu0.03,Dx(D=Y, Gd, Mn) Phosphor Particles Prepared by Spray Pyrolysis. Japanese Journal of Applied Physics, 2008, 47, 163-166.	1.5	6
508	Effects ofN,N-Dimethylacetamide as Drying Control Chemical Additive on Characteristics of Zn2SiO4:Mn,Ba Phosphor Powders Prepared by Spray Pyrolysis. Japanese Journal of Applied Physics, 2008, 47, 7407-7411.	1.5	4
509	Effects of solvent on the properties of nano-sized glass powders prepared by flame spray pyrolysis. Journal of the Ceramic Society of Japan, 2008, 116, 334-340.	1.1	5
510	GdPO4:Tb phosphor particles prepared by spray pyrolysis from the polymeric spray solution. Journal of the Ceramic Society of Japan, 2008, 116, 653-656.	1.1	0
511	Microstructure and electrical properties of nano-sized Ce1-xGdxO2 (0 .LEQ. x .LEQ. 0.2) particles prepared by spray pyrolysis. Journal of the Ceramic Society of Japan, 2008, 116, 969-974.	1.1	6
512	Effects of amide types DCCAs on the properties of Y2O3:Eu phosphor powders with spherical shape and fine size. Journal of the Ceramic Society of Japan, 2008, 116, 955-959.	1.1	1
513	Spherical shape BaNd2Ti5O14 powders prepared by spray pyrolysis. Journal of the Ceramic Society of Japan, 2008, 116, 1289-1294.	1.1	0
514	Nano-sized LaMnO3 powders prepared by spray pyrolysis from spray solution containing citric acid. Journal of the Ceramic Society of Japan, 2008, 116, 141-145.	1.1	9
515	Fine-sized BaMgAl10O17:Eu2+ phosphor powders with plate-like morphology prepared by AlF3 flux-assisted spray pyrolysis. Journal of the Ceramic Society of Japan, 2008, 116, 584-588.	1.1	6
516	Characteristics of nano-sized pb-based glass powders by high temperature spray pyrolysis method. Journal of the Ceramic Society of Japan, 2008, 116, 600-604.	1.1	12
517	Characteristics of TAG:Ce Phosphor Particles Prepared by Ultrasonic Spray Pyrolysis. Solid State Phenomena, 2007, 124-126, 419-422.	0.3	2
518	LiMn2O4 Powders Prepared from Nano-Sized Manganese Oxide Powders. Journal of the Ceramic Society of Japan, 2007, 115, 241-244.	1.3	3
519	Spherical Shape PbO-B2O3-SiO2 Glass Powders Prepared by Flame Spray Pyrolysis. Journal of the Ceramic Society of Japan, 2007, 115, 483-486.	1.1	1
520	Fine Size Cobalt Oxide Powders Prepared by Spray Pyrolysis Using Two Types of Spray Generators. Journal of the Ceramic Society of Japan, 2007, 115, 507-510.	1.1	4
521	Formation of BaMgAl10O17:Eu Phosphor Particles with Spherical Shape and Filled Morphology in the Flame Spray Pyrolysis. Journal of the Ceramic Society of Japan, 2007, 115, 530-535.	1.1	4
522	Fine-sized LiCoO2 Cathode Powders Prepared from the Nano-sized Cobalt Oxide Powders Obtained by Gas Phase Reaction Method. Journal of the Ceramic Society of Japan, 2007, 115, 767-771.	1.1	2

#	Article	IF	CITATIONS
523	Blue-Emitting Eu-Doped (Sr, Mg)5(PO4)3Cl Phosphor Particles Prepared by Spray Pyrolysis from the Spray Solution Containing Ammonium Chloride. Journal of the Ceramic Society of Japan, 2007, 115, 955-959.	1.1	0
524	Effect of preparation temperature on the characteristics of PbO–B2O3–SiO2 glass powders with spherical shape. Journal of Alloys and Compounds, 2007, 428, 344-349.	5.5	20
525	Preparation of Bi2O3–B2O3–ZnO–BaO–SiO2 glass powders with spherical shape by spray pyrolysis. Journal of Alloys and Compounds, 2007, 437, 215-219.	5.5	32
526	Effects of Y/Gd Ratio and Boron Excess on Vacuum Ultraviolet Characteristics and Morphology of (Y,Gd)BO3:Eu Phosphor Particles Prepared by Spray Pyrolysis. Japanese Journal of Applied Physics, 2007, 46, 3424-3427.	1.5	3
527	The characteristics of Li(Ni1/3Co1/3Mn1/3)O2 particles prepared from precursor particles with spherical shape obtained by spray pyrolysis. Ceramics International, 2007, 33, 1093-1098.	4.8	2
528	Preparation of solid nickel nanoparticles by large-scale spray pyrolysis of Ni(NO3)2·6H2O precursor: Effect of temperature and nickel acetate on the particle morphology. Materials Science and Engineering B: Solid-State Materials for Advanced Technology, 2007, 137, 10-19.	3.5	37
529	Fine cathode particles prepared by solid-state reaction method using nano-sized precursor particles. Journal of Power Sources, 2007, 174, 598-602.	7.8	3
530	Fine-sized LiCoO2 particles prepared by spray pyrolysis from polymeric precursor solution. Materials Research Bulletin, 2007, 42, 362-370.	5.2	11
531	The characteristics of the size-controlled Pb-based glass powders with spherical shape. Materials Letters, 2007, 61, 3669-3672.	2.6	7
532	Spherical shape BaO-ZnO-B2O3-SiO2 glass powders prepared by spray pyrolysis. Applied Physics A: Materials Science and Processing, 2007, 89, 769-774.	2.3	8
533	LiMn2O4 particles prepared by spray pyrolysis from spray solution with citric acid and ethylene glycol. Journal of Materials Science, 2007, 42, 5369-5374.	3.7	10
534	Generation of phosphor particles for photoluminescence applications by spray pyrolysis. Journal of Materials Science, 2007, 42, 9783-9794.	3.7	10
535	Al-doped Ni-rich cathode powders prepared from the precursor powders with fine size and spherical shape. Electrochimica Acta, 2007, 52, 7286-7292.	5.2	80
536	Fine cathode particles prepared by solid-state reaction method using nano-sized precursor particles. Journal of Power Sources, 2007, 174, 1161-1166.	7.8	4
537	Synthesis of nanosized Co3O4 particles by spray pyrolysis. Journal of Alloys and Compounds, 2006, 417, 254-258.	5.5	47
538	The characteristics of nano-sized manganese oxide particles prepared by spray pyrolysis. Journal of Alloys and Compounds, 2006, 425, 411-415.	5.5	16
539	PbO–B2O3–SiO2 glass powders with spherical shape prepared by spray pyrolysis. Journal of Non-Crystalline Solids, 2006, 352, 3270-3274.	3.1	39
540	The characteristics of X1 type Y2SiO5:Tb phosphor particles prepared by high temperature spray pyrolysis. Ceramics International, 2006, 32, 865-870.	4.8	18

#	Article	IF	CITATIONS
541	Nano-sized ceria particles prepared by spray pyrolysis using polymeric precursor solution. Materials Science and Engineering B: Solid-State Materials for Advanced Technology, 2006, 127, 99-104.	3.5	58
542	The Effect of flux types on the formation of green light emitting phosphor particles with spherical shape and filled morphology. Journal of Materials Science: Materials in Electronics, 2006, 17, 341-346.	2.2	3
543	Submicron size Li(Ni1/3Co1/3Mn1/3)O2 particles prepared by spray pyrolysis from polymeric precursor solution. Journal of Materials Science: Materials in Electronics, 2006, 17, 353-359.	2.2	9
544	Transparencies of dielectric layers formed from size-controlled Bi-based glass powders obtained by spray pyrolysis. Applied Physics A: Materials Science and Processing, 2006, 85, 63-68.	2.3	26
545	Gd2O3:Eu phosphor particles prepared from spray solution containing boric acid flux and polymeric precursor by spray pyrolysis. Optical Materials, 2006, 28, 530-535.	3.6	24
546	Effect of preparation temperature on the formation of Sr2CeO4 phosphor particles in the spray pyrolysis. Korean Journal of Chemical Engineering, 2006, 23, 496-498.	2.7	1
547	Preparation of CaMgSi2O6:Eu blue phosphor particles by spray pyrolysis and its VUV characteristics. Materials Chemistry and Physics, 2006, 98, 330-336.	4.0	38
548	Fine size Sr2CeO4 phosphor particles prepared by spray pyrolysis from polymeric precursor solution. Materials Letters, 2006, 60, 334-338.	2.6	12
549	Effect of preparation temperature on the characteristics of Eu-doped borate phosphor particles in the spray pyrolysis. Materials Letters, 2006, 60, 3091-3095.	2.6	6
550	Morphology Control of Gd2O3:Eu Phosphor Particles with Cubic and Monoclinic Phases Prepared by High-Temperature Spray Pyrolysis. Japanese Journal of Applied Physics, 2006, 45, 5018-5022.	1.5	10
551	Luminescence Characteristics of Eu-Doped Calcium Magnesium Chlorosilicate Phosphor Particles Prepared by Spray Pyrolysis. Japanese Journal of Applied Physics, 2006, 45, 1617-1622.	1.5	12
552	Direct Synthesis of High-Brightness (CeTb)MgAl11O19Phosphor Particles by Spray Pyrolysis with Boric Acid Flux. Japanese Journal of Applied Physics, 2006, 45, 116-120.	1.5	5
553	Effect of Boric Acid Flux and Drying Control Chemical Additive on the Characteristics of Y2O3:Eu Phosphor Particles Prepared by Spray Pyrolysis. Japanese Journal of Applied Physics, 2006, 45, 9083-9087.	1.5	9
554	Improved thermal resistance of spherical BaMgAl10O17:Eu blue phosphor prepared by spray pyrolysis. Journal of Luminescence, 2005, 115, 91-96.	3.1	24
555	Nano-sized Y2O3:Eu phosphor particles prepared by spray pyrolysis. Materials Science and Engineering B: Solid-State Materials for Advanced Technology, 2005, 116, 59-63.	3.5	26
556	Phosphor layer formed from the Zn2SiO4:Mn phosphor particles with spherical shape and fine size. Materials Science and Engineering B: Solid-State Materials for Advanced Technology, 2005, 117, 210-215.	3.5	32
557	Eu-doped barium strontium silicate phosphor particles prepared from spray solution containing NH4Cl flux by spray pyrolysis. Materials Science and Engineering B: Solid-State Materials for Advanced Technology, 2005, 121, 81-85.	3.5	43
558	Origin of PL intensity increase of CaMgSi2O6:Eu2+ phosphor after baking process for PDPs application. Solid State Communications, 2005, 133, 197-201.	1.9	67

#	Article	IF	CITATIONS
559	Effects of synthesis condition on LiNiMnO cathode material for prepared by ultrasonic spray pyrolysis method. Solid State Ionics, 2005, 176, 481-486.	2.7	54
560	Morphology control and luminescent property of Y3Al5O12:Tb particles prepared by spray pyrolysis. Materials Research Bulletin, 2005, 40, 2212-2218.	5.2	12
561	Y3Al5O12:Tb phosphor particles prepared by spray pyrolysis from spray solution with polymeric precursors and ammonium fluoride flux. Materials Letters, 2005, 59, 2383-2387.	2.6	9
562	Effect of surface area and crystallite size on luminescent intensity of Y2O3:Eu phosphor prepared by spray pyrolysis. Materials Letters, 2005, 59, 2451-2456.	2.6	88
563	Luminescent Properties of (Ba,Sr)MgAl10O17:Mn,Eu Green Phosphor Prepared by Spray Pyrolysis under VUV Excitation ChemInform, 2005, 36, no.	0.0	1
564	Y2SiO5:Tb phosphor particles prepared from colloidal and aqueous solutions by spray pyrolysis. Applied Physics A: Materials Science and Processing, 2005, 80, 347-351.	2.3	16
565	Correlation of photoluminescence of (Y, Ln)VO4:Eu3+ (Ln=Gd and La) phosphors with their crystal structures. Solid State Communications, 2005, 133, 651-656.	1.9	58
566	Effect of Manganese Source Material on Characteristics of Zn2SiO4:Mn Phosphor Particles Prepared by Spray Pyrolysis. Japanese Journal of Applied Physics, 2005, 44, 233-234.	1.5	3
567	(CeTb)MgAl11019Phosphor Particles Prepared by Spray Pyrolysis from Spray Solution Containing Citric Acid and Ethylene Glycol. Japanese Journal of Applied Physics, 2005, 44, 4975-4978.	1.5	10
568	Luminescent Properties of (Ba,Sr)MgAl10O17:Mn,Eu Green Phosphor Prepared by Spray Pyrolysis under VUV Excitation. Chemistry of Materials, 2005, 17, 2729-2734.	6.7	86
569	A Busbar Differential Protection Relay Suitable for Use With Measurement Type Current Transformers. IEEE Transactions on Power Delivery, 2005, 20, 1291-1298.	4.3	33
570	Preparation of nano-sized BaTiO3 particle by citric acid-assisted spray pyrolysis. Journal of Alloys and Compounds, 2005, 395, 280-285.	5.5	60
571	The characteristics of nano-sized Gd-doped CeO2 particles prepared by spray pyrolysis. Journal of Alloys and Compounds, 2005, 398, 240-244.	5.5	28
572	Effect of boric acid flux on the characteristics of (CeTb)MgAl11O19 phosphor particles prepared by spray pyrolysis. Journal of Alloys and Compounds, 2005, 398, 309-314.	5.5	25
573	The enhancement of photoluminescence characteristics of Eu-doped barium strontium silicate phosphor particles by co-doping materials. Journal of Alloys and Compounds, 2005, 402, 246-250.	5.5	29
574	Preparation of Green-Light Emitting BAM:Mn Phosphor Particles by High Temperature Spray Pyrolysis. Korean Journal of Materials Research, 2005, 15, 496-502.	0.2	0
575	Red-Emitting Phosphor Particles with Spherical Shape, Dense Morphology, and High Luminescent Efficiency under Ultraviolet. Japanese Journal of Applied Physics, 2004, 43, 5302-5306.	1.5	16
576	Luminescence and CL Saturation Characteristics of Eu doped Y-Al-O Multicomposition Phosphor Prepared by Spray Pyrolysis. Journal of the Electrochemical Society, 2004, 151, H180.	2.9	7

#	Article	IF	CITATIONS
577	Size-dependent luminescent properties of hollow and dense BaMgAl10O17: Eu blue phosphor particles prepared by spray pyrolysis. Korean Journal of Chemical Engineering, 2004, 21, 1072-1080.	2.7	12
578	Morphology Control and Optimization of Luminescent Property of YBO[sub 3]:Tb Phosphor Particles Prepared by Spray Pyrolysis. Journal of the Electrochemical Society, 2004, 151, H69.	2.9	45
579	Preparation of BaMgAl10017:Eu blue phosphor by flame-assisted spray pyrolysis: photoluminescence properties of powder and film under VUV excitation. Materials Letters, 2004, 58, 2161-2165.	2.6	29
580	Formation of ZnO, MgO and NiO Nanoparticles from Aqueous Droplets in Flame Reactor. Journal of Nanoparticle Research, 2003, 5, 199-210.	1.9	38
581	Title is missing!. Journal of Materials Science Letters, 2003, 22, 1527-1529.	0.5	3
582	Control of size and morphology in Ni particles prepared by spray pyrolysis. Journal of Materials Science Letters, 2003, 22, 1537-1541.	0.5	20
583	Green-emitting yttrium silicate phosphor particles prepared by large scale ultrasonic spray pyrolysis. Korean Journal of Chemical Engineering, 2003, 20, 930-933.	2.7	13
584	Brightness and decay time of Zn2SiO4:Mn phosphor particles with spherical shape and fine size. Applied Physics A: Materials Science and Processing, 2003, 77, 529-532.	2.3	55
585	The synthesis of (Y1-xGdx)2O3:Eu phosphor particles by flame spray pyrolysis with LiCl flux. Applied Physics A: Materials Science and Processing, 2003, 77, 659-663.	2.3	11
586	Y 2 O 3 :Eu phosphor particles prepared by spray pyrolysis from a solution containing citric acid and polyethylene glycol. Applied Physics A: Materials Science and Processing, 2003, 76, 241-245.	2.3	17
587	UV and VUV characteristics of (YGd)2O3:Eu phosphor particles prepared by spray pyrolysis from polymeric precursors. Materials Research Bulletin, 2003, 38, 515-524.	5.2	74
588	Improved photoluminescence of BaMgAl10O17 blue phosphor prepared by spray pyrolysis. Journal of Luminescence, 2003, 105, 127-133.	3.1	43
589	Optimization of VUV characteristics and morphology of BaMgAl10O17:Eu2+ phosphor particles in spray pyrolysis. Ceramics International, 2003, 29, 41-47.	4.8	25
590	Synthesis of Nanosize Gd[sub 2]O[sub 3]:Eu Phosphor Particles with High Luminescence Efficiency under Ultraviolet Light. Journal of the Electrochemical Society, 2003, 150, H93.	2.9	24
591	Morphology of particles prepared by spray pyrolysis from organic precursor solution. Materials Letters, 2003, 57, 1288-1294.	2.6	33
592	Ba[sup 2+] Co-doped Zn[sub 2]SiO[sub 4]:Mn Phosphor Particles Prepared by Spray Pyrolysis Process. Journal of the Electrochemical Society, 2003, 150, H7.	2.9	37
593	VUV characteristics of BaAl12O19:Mn2+ phosphor particles prepared from aluminum polycation solutions by spray pyrolysis. Journal of Alloys and Compounds, 2003, 353, 252-256.	5.5	43
594	Effect of Aluminum Polycation Solution on the Morphology and VUV Characteristics of BaMgAl[sub 10]O[sub 17] Blue Phosphor Prepared by Spray Pyrolysis. Electrochemical and Solid-State Letters, 2003, 6, H27.	2.2	15

#	Article	IF	CITATIONS
595	Morphological Control of Zn2SiO4:Mn Phosphor Particles by Adding Citric Acid in Spray Pyrolysis Process. Japanese Journal of Applied Physics, 2003, 42, 3429-3433.	1.5	22
596	Improved Photoluminescence of Sr[sub 5](PO[sub 4])[sub 3]Cl:Eu[sup 2+] Phosphor Particles Prepared by Flame Spray Pyrolysis. Journal of the Electrochemical Society, 2003, 150, H38.	2.9	23
597	Vacuum Ultraviolet Characteristics of Nano-sized Gd2O3:Eu Phosphor Particles. Japanese Journal of Applied Physics, 2003, 42, 2741-2745.	1.5	22
598	Preparation of Layered Li[Ni1/2Mn1/2]O2by Ultrasonic Spray Pyrolysis Method. Chemistry Letters, 2003, 32, 446-447.	1.3	11
599	Vacuum Ultraviolet Characteristics of Fine GdPO4:Tb Phosphor Particles With Spherical Shape. Japanese Journal of Applied Physics, 2002, 41, 5590-5593.	1.5	14
600	ZnGa2O4:Mn Phosphor Particles with Spherical Shape and Clean Surface. Japanese Journal of Applied Physics, 2002, 41, 4559-4562.	1.5	8
601	Morphological Control of Y2O3:Eu Phosphor Particles by Adding Polymeric Precursors in Spray Pyrolysis. Japanese Journal of Applied Physics, 2002, 41, 3006-3009.	1.5	58
602	(YGd)BO3:Eu Phosphor Particles Prepared from the Solution of Polymeric Precursors by Spray Pyrolysis. Japanese Journal of Applied Physics, 2002, 41, 6007-6010.	1.5	4
603	Precursor Type Influence on the Morphology and VUV Characteristics of GdPO[sub 4]:Tb Phosphor Particles Prepared by Spray Pyrolysis. Electrochemical and Solid-State Letters, 2002, 5, H31.	2.2	9
604	High brightness LaPO4:Ce,Tb phosphor particles with spherical shape. Journal of Alloys and Compounds, 2002, 347, 266-270.	5.5	88
605	Direct synthesis of strontium titanate phosphor particles with high luminescence by flame spray pyrolysis. Materials Research Bulletin, 2002, 37, 263-269.	5.2	40
606	Use of LiCl flux in the preparation of Y2O3:Eu phosphor particles by spray pyrolysis. Journal of the European Ceramic Society, 2002, 22, 1661-1665.	5.7	46
607	High luminescence Y2O3 : Eu phosphor particles prepared by modified spray pyrolysis. Journal of Materials Science Letters, 2002, 21, 1027-1029.	0.5	12
608	One-step synthesis of the green phosphor Ce-Tb-Mg-Al-O system with spherical particle shape and fine size. Applied Physics A: Materials Science and Processing, 2001, 72, 103-105.	2.3	11
609	Luminescence Characteristics of Eu-doped Strontium Halophosphate Phosphor Particles Prepared by Spray Pyrolysis. Japanese Journal of Applied Physics, 2001, 40, 3222-3225.	1.5	8
610	Morphological and Optical Characteristics of Y2O3:Eu Phosphor Particles Prepared by Flame Spray Pyrolysis. Japanese Journal of Applied Physics, 2001, 40, 4083-4086.	1.5	50
611	Gd[sub 2]O[sub 3]:Eu Phosphor Particles Prepared from the Polymeric Precursors in Spray Pyrolysis. Journal of the Electrochemical Society, 2001, 148, H171.	2.9	20
612	Sodium Carbonate Flux Effects on the Luminescence Characteristics of (Y <sub>0.5</sub> Gd <sub>0.5</sub> ) <sub>2</sub> O <sub>3</sub> :Eu Phosphor Particles Prepared by Spray Pyrolysis. Journal of the American Ceramic Society, 2001, 84, 447-49.	3.8	30

#	Article	IF	CITATIONS
613	Preparation of Y2O3:Eu Phosphor Particles of Filled Morphology at High Precursor Concentrations by Spray Pyrolysis. Advanced Materials, 2000, 12, 451-453.	21.0	196
614	Morphology and Luminescence of(GdY)2O3:Eu Particles Prepared by Colloidal Seed-Assisted Spray Pyrolysis. Journal of Colloid and Interface Science, 2000, 228, 195-199.	9.4	29
615	YAG:Ce phosphor particles prepared by ultrasonic spray pyrolysis. Materials Research Bulletin, 2000, 35, 789-798.	5.2	213
616	Zn2SiO4:Mn phosphor particles prepared by spray pyrolysis using a filter expansion aerosol generator. Materials Research Bulletin, 2000, 35, 1143-1151.	5.2	92
617	Title is missing!. Journal of Materials Science Letters, 2000, 19, 1225-1227.	0.5	17
618	Morphology Control of BaMgAl[sub 10]O[sub 17]:Eu Particles: The Use of Colloidal Solution Obtained from Alkoxide Precursor in Spray Pyrolysis. Journal of the Electrochemical Society, 2000, 147, 799.	2.9	42
619	The Effect of Metal Chloride Fluxes on the Properties of Phosphor Particles in Spray Pyrolysis. Japanese Journal of Applied Physics, 2000, 39, L1305-L1307.	1.5	12
620	Morphology of Oxide Phosphor Particles Prepared by Colloidal Seed-Assisted Spray Pyrolysis. Journal of the Electrochemical Society, 2000, 147, 1601.	2.9	30
621	Improvement of Brightness of Gd2O3:Eu Phosphor Particles Using Boric Acid Flux in the Spray Pyrolysis. Japanese Journal of Applied Physics, 2000, 39, L31-L33.	1.5	14
622	Photoluminescence Properties of Ce1-xTbxMgAl11O19Phosphor Particles Prepared by Spray Pyrolysis. Japanese Journal of Applied Physics, 1999, 38, 2013-2016.	1.5	8
623	Morphology of (YxGd1-x)BO3:Eu Phosphor Particles Prepared by Spray Pyrolysis from Aqueous and Colloidal Solutions. Japanese Journal of Applied Physics, 1999, 38, L1541-L1543.	1.5	33
624	Morphology Control of Multicomponent Oxide Phosphor Particles Containing High Ductility Component by High Temperature Spray Pyrolysis. Journal of the Electrochemical Society, 1999, 146, 2744-2747.	2.9	36
625	Luminescence Characteristics of  Y 2SiO5 : Tb Phosphor Particles Directly Prepared by the Spray Method. Journal of the Electrochemical Society, 1999, 146, 1227-1230.	Pyrolysis	87
626	Preparation of nonaggregated Y <sub>2</sub> O <sub>3</sub> : Eu phosphor particles by spray pyrolysis method. Journal of Materials Research, 1999, 14, 2611-2615.	2.6	90
627	Gd2O3:Eu phosphor particles with sphericity, submicron size and non-aggregation characteristics. Journal of Physics and Chemistry of Solids, 1999, 60, 379-384.	4.0	138
628	Photoluminescence characteristics of YAC:Tb phosphor particles with spherical morphology and non-aggregation. Journal of Physics and Chemistry of Solids, 1999, 60, 1855-1858.	4.0	111
629	Submicron-Size BaAl12O19:Mn Phosphor Particles with Spherical Morphology. Journal of Materials Science Letters, 1999, 18, 779-781.	0.5	14
630	Y2SiO5:Ce Phosphor Particles 0.5–1.4 μm in Size with Spherical Morphology. Journal of Solid State Chemistry, 1999, 146, 168-175.	2.9	42

#	Article	IF	CITATIONS
631	Preparation of zinc oxide-dispersed silver particles by spray pyrolysis of colloidal solution. Materials Letters, 1999, 40, 129-133.	2.6	31
632	Preparation of YAG:Europium Red Phosphors by Spray Pyrolysis Using a Filterâ€Expansion Aerosol Generator. Journal of the American Ceramic Society, 1999, 82, 2056-2060.	3.8	50
633	Preparation of high surface area Mgal2O4 particles from colloidal solution using filter expansion aerosol generator. Journal of the European Ceramic Society, 1998, 18, 641-646.	5.7	11
634	Formation of Submicron Copper Sulfide Particles Using Spray Pyrolysis Method. Japanese Journal of Applied Physics, 1998, 37, L288-L290.	1.5	23
635	Photocatalytic activity of nanometer size ZnO particles prepared by spray pyrolysis. Journal of Aerosol Science, 1997, 28, S473-S474.	3.8	55
636	Preparation of CaTiO3:Pr phosphor by spray pyrolysis using filter expansion aerosol generator. Journal of Aerosol Science, 1997, 28, S541-S542.	3.8	25
637	Preparation of perovskite-type La0.85Sr0.15MnO3 particles by spray pyrolysis using a filter expansion aerosol generator. Journal of Materials Science Letters, 1997, 16, 1201-1204.	0.5	3
638	Title is missing!. Journal of Materials Science Letters, 1997, 16, 1201-1204.	0.5	2
639	Title is missing!. Journal of Materials Science Letters, 1997, 16, 1848-1849.	0.5	32
640	Title is missing!. Journal of Materials Science Letters, 1997, 16, 131-133.	0.5	30
641	Preparation of Submicron Size Gamma Lithium Aluminate Particles from the Mixture of Alumina Sol and Lithium Salt by Ultrasonic Spray Pyrolysis. Journal of Colloid and Interface Science, 1996, 182, 59-62.	9.4	30
642	Preparation of nanometre size oxide particles using filter expansion aerosol generator. Journal of Materials Science, 1996, 31, 2409-2416.	3.7	37
643	Preparation of high surface area nanophase particles by low pressure spray pyrolysis. Scripta Materialia, 1995, 5, 777-791.	0.5	30
644	A high-volume spray aerosol generator producing small droplets for low pressure applications. Journal of Aerosol Science, 1995, 26, 1131-1138.	3.8	58
645	Electrochemical properties of sulfur–carbon hollow nanospheres with varied polar titanium oxide layer location for lithium–sulfur batteries. International Journal of Energy Research, 0, , .	4.5	3